Modifying Prion Disease Development by Ablation of Galectin-3 and by Simvastatin-Treatment

A Dissertation

Submitted in Partial Fulfilment of the Requirements for the Degree of

Doctor rerum naturalium (Dr.rer.nat)

to the Department of Biology, Chemistry and Pharmacy

of Freie Universität Berlin

by

Simon Wing-Fai Mok

from Hong Kong SAR, China

Berlin, December 2011

Supervisor : Prof. Dr. Kürşad Turgay

Second examiner : Prof. Dr. Reinhard Geβner

Date of the viva voce/defense: 12/10/2009

Acknowledgements

After the four years of staying in Berlin and studying in the Project Group ‘’Neurodegenerative Diseases’’ (P23), I wish to thank a number of people for their encouragement and support.

First, I would like to send my scincere gratitude to my supervisor Dr. Michael Baier for proividing me guidance throughout the studies, and most importantly, giving me the freedom to explore on my own.

I would also like to thank Dr. Contanze Riemer for her advice on my studies and assistance during the preparation of this dissertation.

I am thankful to Mrs. Lichy Mrs. Westhäuser for providing the assistance and preparing the materials for my work. My thanks also go out to Mrs. Krohn for teaching me patiently the experimental techniques and the German language.

I am also indebted to my colleague, Sandra Gütlner, Ines Heise, Ina Zobel, Jaehoon You, Silke Tröller and Ute Kraff for their friendships which help adjusting myself to the new country and culture.

Also, I am grateful for the support and care from the Wai’s family, which helped me stay sane through the difficult times both in studies and living.

At last, I would like to express my depeest gratitude to my parents and brothers. Without their encouragement, my work in Berlin would not be successful. Thank you for their encouragement, and loves which is of great importane to me to overcome setbacks and stay focused on my graduate study.

Declaration

This project was conducted and finished in project group 23 (P23) ‘’Neurodegenerative Diseases’’ in the Robert-Koch Institut under the supervision of Dr. Michael Baier. This thesis is submitted to the Department of Biology, Chemistry and Pharmacy of Freie Universität Berlin to obtain the academic degree of Doktor der Naturwissenschaften (Dr. rer. nat). It has not been submitted for any other degree of any examining body. Except where specifically mentioned, it is all the work of the author.

Berlin

Summary

Galectin-3 is highly overexpressed in prion-infected brain tissue. Immunofluorescence double-labelling identified microglia as the major cell type expressing galectin-3. Ablation of galectin-3 did not affect PrP^{Sc}-deposition and development of gliosis. However, galectin-$3^{-/-}$-mice showed prolonged survival times upon intracerebral and peripheral scrapie infections. Moreover, protein levels of the lysosomal activation marker LAMP-2 were markedly reduced in prion-infected galectin-$3^{-/-}$-mice suggesting a role of galectin-3 in regulation of lysosomal functions. Lower mRNA levels of Beclin-1 and Atg5 in prion-infected wild-type and galectin-$3^{-/-}$-mice point towards a possible impairment of autophagy. However, LC3-II/LC3-I ratios remained unchanged in uninfected and scrapie-infected WT- or galectin-$3^{-/-}$-mice indicating no general increase or decrease of autophagosome numbers. The results point towards a detrimental role of galectin-3 in prion infections of the CNS and suggest that endo-/lysosomal dysfunction in combination with reduced autophagy may contribute to disease development.

The second part of this study addressed the potential of the cholesterol-lowering drug simvastatin for therapeutic intervention in a murine prion disease model. Statins have been reported to inhibit prion replication in cell cultures and to modulate inflammatory reactions. Groups of mice were intracerebrally infected with two doses of scrapie strain 139A. Simvastatin-treatment commenced 100 days postinfection. The treatment did not affect deposition of misfolded prion protein PrP^{Sc}. However, expression of marker proteins for glia activation like major histocompatibility complex class II and galectin-3 was found to be affected. Analysis of brain cholesterol synthesis and metabolism revealed a mild reduction in cholesterol precursor levels, whereas levels of cholesterol and cholesterol metabolites were unchanged. Simvastatin-treatment significantly delayed disease progression and prolonged survival times in established prion infection of the CNS ($p<0003$). Overall, these results suggests that the therapeutic benefit of simvastatin observed in our murine prion model is not due to the cholesterol-lowering effect of this drug. Taken together, the findings from both studies highlight the significant role of prion-induced inflammatory responses in the CNS in disease development and encourage use of immunomodulatory/anti-inflammatory drugs for therapeutic intervention in prion diseases.

Zusammenfassung

In Prion-infiziertem Hirngewebe zeigt Galektin-3 eine starke Überexpression. Mit Hilfe von Doppelfärbungen wurden Mikrogliazellen immunhistochemisch als Galektin-3 exprimierender Zelltyp identifiziert. Galektin-$3^{-/-}$-Mäuse zeigten nach intrazerebraler und peripherer Scrapie-Infektion eine verlängerte Überlebenszeit. Die Abwesenheit von Galektin-3 beeinflusste jedoch weder PrP^{Sc}-Ablagerungen noch die Entwicklung der Gliose. LAMP-2, ein Biomarker der lysosomalen Aktivität, zeigte hingegen eine deutlich verringerte Proteinexpression in Galektin-$3^{-/-}$-Mäusen, was auf einen möglichen Einfluss von Galektin-3 auf lysosomale Funktionen hinweist. Verminderte mRNA-Level von Beclin-1 und Atg5 in Prion-infizierten Wildtyp- und Galektin-$3^{-/-}$-Mäusen deuten auf eine Beeinträchtigung des Autophagie-Systems hin. Die Untersuchung der LC3-II/LC3-I Mengenverhältnisse ergab jedoch keinen Hinweis auf eine generelle Ab- oder Zunahme an Autosomen. Die Ergebnisse zeigen die schädliche Rolle des Galektin-3 bei Prion-Infektionen des ZNS, wobei eine endo-/lysosomale Dysfunktion in Kombination mit einer reduzierten Autophagie zur Krankheitsentwicklung beiträgt.

Der zweite Teil dieser Arbeit beschäftigte sich mit dem therapeutischen Potential des Cholesterin-senkenden Wirkstoffs Simvastatin im murinen Prionmodell. Für Statine ist die Modulation von inflammatorischen Reaktionen und die Inhibition der Prion-Replikation in der Zellkultur beschrieben. Versuchsgruppen von Mäusen wurden mit zwei verschiedenen Infektionsdosen des Scrapie-Stammes 139A intrazerebral infiziert und 100 Tage nach Infektion mit Simvastatin behandelt. Die Behandlung hatte keinen Einfluss auf die Ablagerung des umgefalteten Prion-Proteins PrP^{Sc}, jedoch war die Expression der Gliaaktivierungsmarker MHC II (major histocompatibility complex class II) und Galektin-3 verändert. Analysen von Cholesterinsynthese und –metabolismus im Gehirn zeigten leicht reduzierte Konzentrationen von Cholesterinvorläufern aber unveränderte Konzentrationen von Cholesterin und Cholesterinmetaboliten. Die Simvastatinbehandlung führte zu einer Verzögerung des Krankheitsverlaufs und einer signifikant verlängerten Überlebenszeit bei bestehender Prion-Infektion des ZNS ($p<0,01$). Insgesamt deuten die Ergebnisse darauf hin, dass der therapeutische Effekt von Simvastatin in unserem murinen Prion-Modell wahrscheinlich nicht auf dessen Cholesterin-senkende Wirkung zurückzuführen ist. Zusammengefasst weisen die Ergebnisse beider Teile dieser Arbeit auf die Bedeutung der Prion-induzierten inflammatorischen Reaktion im ZNS in der Pathogenese von Prion-Krankheiten hin und lassen

den Einsatz von immunmodulatorischen/anti-inflammatorischen Wirkstoffen zur therapeutischen Intervention als sinnvoll erscheinen.

Table of Content

1 Introduction

Prion diseases are fatal disorders of the central nervous system (CNS). Their infectious nature is unique amongst neurodegenerative protein misfolding diseases. Vacuolization of brain tissues and neuronal degeneration are typical consequences of prion infections. With these observations, prion diseases are also called transmissible spongiform encephalopathy (TSE). As proposed by Stanley B. Prusiner in 1982, the term "prion" refers to the pathogen, PrP^{Sc}, a conformational isomer of the cellular prion protein PrP^{c}, being **pro**teinaceous and **in**fectious [1].

1.1 Prion Diseases in Human and Other Species

Scrapie, the earliest recorded prion disease, was discovered in sheeps in the 18th century Europe and is still affecting ovine species nowadays [2]. Prion diseases are also found in a variety of mammals. Some examples are the infamous bovine spongiform encephalopathy (BSE), feline spongiform encephalopathy (FSE), transmissible mink encephalopathy (TME), as well as chronic wasting disease (CWD) in elk and deer, which is spreading rapidly in North America [3, 4]. Among these, BSE is of particular interest because of its possible infectivity towards humans.

The human equivalent, Creutzfeldt-Jacob Disease (CJD), was first described in the 1920s by two German medical doctors Hans G. Creutzfeldt and Alfons M. Jakob [5, 6]. It is mainly sporadic in nature and is a rare disease with an incidence of around one case per million people per year [7]. The first record of human prion disease establishing an epidemic proportion was Kuru in Papua New Guinea, which was believed to be related to ritual cannibalism in these regions [8, 9]. It was proven to be infectious after being experimentally transmitted to chimpanzees [10]. In the mid-90s, the variant Creutzfeldt-Jacob Disease (vCJD), likely to be caused by BSE-contaminated food products, was reported in the UK [7, 11-13]. Although only about 200 people have died from vCJD to date (http://www.cjd.ed.ac.uk/vcjdworld.htm), the numbers of subclinical carriers are still unknown. Thus, they may become potential sources of iatrogenic contamination of materials such as cornea/dura matter transplants or surgical instruments.

Apart from acquired cases, familial prion diseases like Gerstmann-Sträussler-Scheinker-Syndrome (GSS) and fatal familial insomnia (FFI) which are caused by autosomal dominant mutations of the PrP^{c} encoding gene, prion protein gene (*PRNP*) have also been documented

[14-16]. Interestingly, non-pathogenic *PRNP* polymorphism have also been described suggesting differential susceptibility to the disease in relation to genetic contributions [17-22].

1.2 The Prion Protein

1.2.1 The Cellular Isoform of Prion Protein (PrP^c)

PrP^c is a membrane glycoprotein and its encoding gene, *PRNP*, is highly conserved amongst a variety of species [23]. *PRNP* mRNA is detected in lymphocytes, leukocytes, and different types of neurons including neocortical-, hippocampal- neurons and cerebellar Purkinje cells, as well as glial cells in the CNS [24-28]. PrP^c is a protein of 253 amino acids containing a signal peptide at the amino terminal followed by octapetide repeats. As post-translational modifications, the signal peptide is removed and the protein is subjected to N-linked glycosylation (CHO) and the addition of a glycosylphosphatidylinositol (GPI) anchor at the carboxyl terminal end. As cell surface protein, it is believed to be localized in glycosphingolipid- and cholesterol-rich rafts [29-31].

The highly conserved structure of PrP^c amongst different species implies vital roles of the protein in fundamental biological processes. It is hypothesized to be part of transmembrane signaling pathways because of its location on the well-known signal transduction-mediating platform, rafts [32, 33]. The involvement of PrP^c in mediating cellular signaling is further supported by *in vitro* tests mimicking the actions of PrP^c ligands by cross-linking cell surface PrP^c with different antibodies [34, 35]. Other evidences for PrP^c-mediated signal transductions have also been observed using *PRNP* knockout animals and cell cultures treated with recombinant PrP [36, 37]. Besides, PrP^c may also have a functional role in synaptic integrity by regulating synapse formation and synaptic transmission [38, 39]. The fact that synaptic abnormality appears to be the prominent feature in prion diseases indirectly indicates the importance of the protein at synapses [40, 41]. Furthermore, PrP^c appears to be neuroprotective as neuron cultures from *PRNP* knockout mice were more susceptible to oxidative stress [42-45]. It was hypothesized that this could be related to the anti-apoptotic property of the protein influencing caspase-dependent apoptotic pathways in mitochondria [44]. In addition, PrP^c has a copper-binding domain at its octapeptide repeats and may serve as a receptor for cellular uptake of copper ions [46-51].

1.2.2 The Disease Associated Form of Prion Protein (PrP^{Sc}) and Prion Propagation

PrP^{Sc} is a β-sheet enriched structure containing 45% β-sheet and 30% α-helix [52]. According to the protein-only hypothesis, PrP^{Sc} is postulated to be the essential and sufficient component responsible for the autocatalytic conversion from the α-helix-rich cellular PrP^{c} [53]. Dramatic alterations of both physical and chemical properties occur as a result: PrP^{c} is a soluble protein sensitive to proteases and ultra-violet (UV), while PrP^{Sc} is insoluble and protease- and UV-resistant [1]. Such changes are crucial since differential infection patterns of various PrP^{Sc} strains could be explained by different tertiary conformations identified based on protease sensitivity [54]. Several models have been proposed in the attempt to explain the propagation of PrP^{Sc}. One of the hypotheses is the heterodimers model where PrP^{Sc} monomer serves as the template for the conformational changes of PrP^{c} through the formation of PrP^{c}/PrP^{Sc}-dimmers [55]. However, the nucleation-polymerization model emphasized that PrP^{Sc} monomer alone is unstable to act as a template. Instead, oligomeric PrP^{Sc} is required for binding and stabilizing the PrP^{c}/PrP^{Sc} equilibrium [56]. Increasing findings suggest the presence of other additional host-encoded molecules for PrP^{c} conversion [57-60]. In particular, protein X may serve as chaperone to facilitate the conversion process by partially unfolding PrP^{c} into an intermediate called PrP^{*} [61, 62]. Furthermore, it is believed that lipid rafts act as a platform allowing PrP^{c} and PrP^{Sc} to be in close proximity for interactions [63-65]. Nevertheless, further studies are warranted to elucidate the mechanisms of protein conversion.

1.3 Pathogenesis of Prion Diseases

1.3.1 Role of Immune System and Peripheral Prion Transmission

While the exact identity of the source of prion diseases is unclear, consumption of prion-contaminated food products appears to be one of the main routes of human and livestock acquisition of prion. It is known that the immune system plays an essential role in peripheral transmission of prion to the CNS. In most species, gut-associated lymphoid tissue (GALT) is the main site of uptake of orally ingested PrP^{Sc} indicated by the early increased infectivity at distal ileum where Peyer's patches are densely located [66]. *In vitro* studies further suggested M-cells located within the epithelium of Peyer's patches as the entrance of acquired prion [67]. M-cells are specialized epithelial cells on the intestinal epithelium for transepithelial transportation of macromolecules and particles. Apart from Peyer's patches, the isolated

lymphoid follicle (ILF) also appears to be another site for prion uptake [68]. After intestinal absorption of PrP^{Sc}, it is transported to other peripheral lymphoid organs including the spleen. The follicular dendritic cells (FDCs) localized in the germinal centers (GCs) of these organs are the key replication sites for the invading PrP^{Sc} [69]. PrP^{Sc} accumulates both on the plasmalemma and within the extracellular spaces around the dendrites on FDCs [40]. Such binding may be facilitated by opsionization of the protein with complement components like C1q [70]. Other cellular components of the immune system also participate in this process by maintaining the proper functioning of FDCs. Tumor necrosis factor-α (TNF-α) and lymphotoxin-β (LT- β), released by B-cells to regulate the maturation of FDCs, are important in this process [71-73]. Interestingly, T-cells despite being one of the main immune cell types within lymphoid tissues, have no significant role in prion pathogenesis. In a process called neuroinvasion, PrP^{Sc} is transmitted from the peripheral lymphoid organs to the CNS through the neighboring PrP^{c}-expressing sympathetic nerve [74]. However, the precise cell types involved in this process are still unclear.

1.3.2 The Prion Infected Central Nervous System

Vacuolization of neurons and neuropils, as well as, aggregation of PrP^{Sc} in glia and neurons in prion-infected CNS are characteristic pathologies of prion infected CNS [53, 75-77]. While it is suggested that prion-induced neural death is related to both apoptosis and necrosis [78], recent findings also point towards the possible involvement of autophagy [79, 80]. However, the precise mechanisms contributing to the ultimate neural death are still elusive. Several lines of evidences point towards the detrimental effects of PrP^{Sc} and the loss of normal PrP^{c} functions.

PrP^{c} has a potential neuroprotective role in the CNS (section 1.2.1). Since the continuous accumulation of PrP^{Sc} results in a progressive conversion of PrP^{c} into the misfolded isoform, neurotoxicity could be mediated by the loss of normal PrP^{c} functions. On the other hand, it has been demonstrated that PrP-derived peptides and purified PrP^{Sc} are able to directly induce apoptotic and/or necrotic cell death [81-84]. However, other findings suggested that PrP^{Sc}-mediated neurotoxicity may be associated with other cellular components, for example, microglia [85, 86].

Extensive gliosis preceding neurodegeneration is also a characteristic histopathology following prion infection [76]. This chronic gliosis is associated with the subsequent release and

generation of neurotoxic factors, as well as, the regulation of extracellular glutamate homeostasis [76, 87-89]. Glutamate is a major neurotransmitter released by cerebellar cells [90]. Astrocytes are responsible for clearance of excessive extracellular glutamate, which is potentially neurotoxic [91]. However, proliferating astrocytes are not efficient in glutamate uptake. *In vitro* studies demonstrated that $PrP^{106-126}$ promoted proliferation of astrocytes thus inhibited the astrocytic glutamate uptake [92-94]. Therefore, astrocytosis could indirectly affect neuronal survival after prion infection. This prion-induced proliferation of astrocytes also depends on the cytokines released from microglia [95].

$PrP^{106-126}$ can activate microglia and stimulate the release of IL-1, IL-6 and TNF-α *in vitro* [93, 96]. Microglia extend their processes around the rim of vacuoles and the periphery of amyloid plaques [97]. These are strong evidence suggesting that inflammatory response involving microglia may have significant roles in prion pathogenesis. Interestingly, neither B nor T cells appeared to be active participants in the prion infected CNS[98-100]. However, overexpresssion of TNF-α, IL-1α, IL-1β, IL-6, TGFβ1, CXCL10, and CXCL13 by activated glial cells detected in scrapie-infected brain tissues indicated an involvement of cytokines [76, 101-105]. While IL-1 and IL-6 are required for $PrP^{106-126}$-induced astrocyte proliferation, *in vivo* tests further suggested the detrimental effects of scrapie-induced IL-1 in promoting astrocytosis at the asymptomatic stage of the disease [95, 106]. On the other hand, it could not be ruled out that inflammatory mediators could directly induce neurotoxicity as demonstrated for CXCL10 *in vitro* [107]. Details of the communication between the different cells types *in vivo* through these factors are not fully understood.

Another function of microglia in innate immunity is phagocytosis [108]. Macrophages in spleen have demonstrated the ability to clear off scrapie inoculum delivered intraperitoneally [109]. Whether or not microglia in the prion-infected CNS is performing the same should be further clarified, even though indirect evidence has been observed in some scrapie strains [110, 111]. Apart from the release of cytokines and chemokines, upregulation of different cell surface antigens and cytosolic proteins like MHC-II, CR3 and galectin-3 is another response of activated microglia/macrophages [112, 113].

1.4 Galectin-3

1.4.1 The Galectin Family

Galectins, a family of proteins present in many species, are characterized by conserved carbohydrate-recognition domain (CRD) containing approximately 130 amino acids and binds specifically to β-galactosides shown in cases where Galβ1 binds to 4Glc and 4GlcNAc β1 [114]. At present, 15 mammalian members have been identified and the number of potential candidates is increasing [114, 115]. Known members contain at least one CRD and show different binding specificity towards β-galactosides depending on the glycan structures [116]. Galectins lack signal sequence for secretion from the endoplasmic reticulum (ER) suggesting other forms of secretion [117-119]. Based on the number of CRD and protein structure, galectins are further classified into three subgroups: proto-, chimera-, and tandem-repeat-types [120].

1.4.2 Characteristics and Biosynthesis of Galectin-3

Galectin-3, a 29- to 35-kDa protein, was initially identified as antigen Mac-2 expressed on the surface of murine thioglycollate-elicited macrophages [121]. The structure of galectin-3 appears to be unique among all vertebrate galectins [122]. Despite the lack of any signal sequence, galectin-3 is found in extracellular matrix and predominantly located in cytoplasm and other sub-cellular compartments [119, 123]. Ectocytosis, a non-classical secretion pathway bypassing the ER and golgi body (GB), has been suggested as a potential process for extracellular delivery of galectin-3 [118, 124]. It is believed that by doing so, premature binding of galectin-3 to other conventionally secreted glycoproteins can be avoided [125]. The whole CRD is located in the C-terminus and contributes mainly to the lectin property of galectin-3. In addition to the recognition of specific lactosamines, the C-terminus can interact with specific molecules motifs like the NWGR sequence of Bcl-2 family proteins [126-131]. The N-terminal domain is important for signalling the non-classical secretion pathways and has been suggested to participate in the C-terminal-CRD-mediated oligosaccharide binding process [132, 133].

1.4.3 Functions and Immunomodulatory Effects of Galectin-3

Galectin-3 is a multi-functional protein produced by a wide range of tissues such as epithelium of different organs [134-136]. It is also expressed in the cells involved in immune response, such as neutrophils, eosinophils, basophils mast cells, as well as monocytes/macrophages [137-

142]. Its association with cell growth, apoptosis and cellular differentiation has also been demonstrated [143]. Endogenous galectin-3 is generally localized in both cytoplasm and nucleus depending on cell types and proliferative [144-148]. In the cytoplasm, galectin-3 is involved in different intracellular events like apoptosis, proliferation and differentiation. Bcl-2 is one of the binding partners of galectin-3 that is involved in apoptosis [131]. Other binding partners include CD95 (APO-1/Fas), Nucling and Alix/AIP1, K-Ras- and Akt-protein [149-154]. In the nucleus, galectin-3 modulates cellular physiology by regulating gene transcriptions through binding with different transcription factors [155]. CRE and Sp1, the promoters for the cell cycle regulating gene cyclin D_1 have been found as interacting partners with galectin-3 [155]. Galectin-3 also acts as a pre-mRNA splicing factor through the participation in the formation of SMN containing complexes, which are required for pre-mRNA splicing in the pathway of spliceosome assembly [156, 157].

Secreted galectin-3 is involved in cell/cell adhesion and in adhesion to extracellular matrices via cell surface glycoconjugates [151, 158]. It also promotes migration of human monocytes and macropahges through interactions with surface antigens like integrins α1β1 and Mac-1 [158-160]. In addition to its role as chemoattractant in the immune system, exogenous galectin-3 contributes extensively in the homeostasis and activation of these cells. T- and B-cells survival is modulated by the interactions between galectin-3 and receptors/cellular components on these cells which trigger the downstream apoptotic signalling pathways [161, 162]. In addition, activation of the immune cells can be mediated by triggering a cascade of signalling events through the cross-linking of extracellular galectin-3 with specific carbohydrate moieties of glycoprotein/glycolipid membrane receptors on these cells [138, 163]. On the other hand, this cross-linking can also downregulate cellular activation through the formation of membrane surface complex that render the mobility of surface receptors, for example, the repression of T-cell receptor (TCR) signalling [164, 165].

The carbohydrate binding property of galectin-3 is important for recognizing the galactoside-containing glycoconjugates on pathogens [166]. Galectin-3 serves as pattern recognition receptor (PRR) for pathogen associated molecular patterns (PAMPs) like LPS from certain bacteria [167]. The N-terminus of galectin-3 could also play a role in pathogens recognition [168].

Galectin-3 was found to be associated with the phagosomal membrane of mycobacterium infected macrophages suggesting its potential role in influencing phagocytosis [169]. Mice deficient in galectin-3 (galectin-$3^{-/-}$) showed attenuated phagocytic clearance of apoptotic thymocytes by peritoneal macrophages [170]. In addition, it is involved in the phagocytosis of degenerated myelin in experimental allergic encephalomyelitis (EAE) [171]. However, the precise mechanism of the involvement of galectin-3 in phagocytosis remains to be elucidated.

Recent *in vivo* studies of galectin-$3^{-/-}$ mice revealed attenuated peritoneal inflammatory responses and airway hyperresponsiveness suggesting a pro-inflammatory function of this protein in immune response [172, 173]. Incidentally, galectin-3 is also present in peripheral nervous system (PNS) and CNS neurons, Schwann cells, astrocytes, microglia and even gliomas [174-176]. However, functional insights into galectin-3 biology in the nervous system are as yet at best sketchy.

1.5 Therapy of Prion Diseases

1.5.1 Strategies for therapeutic method

Owing to the central role of misfolded prion protein in the disease development, PrP^{Sc} aggregation and propagation appear to be the most rational therapeutic targets in human TSEs. Therefore, methods targeting PrP^{c} could prevent disease progression. This idea is supported by loss of PrP^{Sc} accumulation in vitro as a result of RNA interference targeting the *PRNP* gene [177]. In addition, neuron-specific *PRNP* depletion after established prion infection reversed the early spongiform changes leaving the mice asymptomatic [178].

Apart from regulating neuronal endogenous PrP^{c} levels, modulating the PrP^{c}/PrP^{Sc} interactions would be another feasible therapeutic strategy. Both *in vitro* and *in vivo* studies suggested that monoclonal antibodies like 6H4 which bind to specific portion of PrP^{c} could inhibit PrP^{Sc} accumulation [179, 180]. By doing so, interactions between PrP^{c} and PrP^{Sc} were hindered which subsequently inhibited conversion and propagation processes. While other substances that inhibit PrP^{Sc} aggregation and replication have also been reported, most of them are only effective in prion-infected cultures but are completely ineffective against prion infections *in vivo* [181-185]. In particular, compounds like statins have been described to prevent prion accumulation *in vitro* [186]. Their *in vivo* effect has not yet been extensively studied.

1.5.2 The Statin Family and Simvastatin

Statins, well known cholesterol-lowering drugs, are first-line therapy in the treatment of cholesterol-induced atherosclerotic-cardiovascular diseases. As 3-hydroxymethyl-3-glutaryl coenzyme A reductase (HMG-CoAR) inhibitors, they are structural analogs of mevalonate and affect the rate-limiting step in cholesterol biosynthesis cascade. Statins inhibit the conversion of HMG-CoA to mevalonate by competitive blocking of the responsible enzyme, HMG-CoAR. The endogenous cholesterol synthesis in the liver is reduced and, consequently, levels of circulating LDL-cholesterol are decreased due to the increasing number of LDL-receptors on cell surfaces [187]. Apart from the cholesterol lowering ability, statins have recently attracted considerable interest due to their immunomodulatory and anti-inflammatory properties [188-190]. Simvastatin, commercially available as Zocor, is a lipophilic member of the statins family and can pass through the blood brain barrier (BBB). It is a relatively safe prescription drug for patients with coronary heart disease and high cholesterol. In addition, it has also been reported to minimize the risk of stroke or transient ischemic attack (TIA) [191]. Given its established modulatory effect on inflammation and the involvement of inflammatory responses in prion disease, the potential of simvastatin for therapeutic oral intervention needs to be explored.

2 Objectives of the Study

Increasing evidence suggested the significance of inflammatory components in the prion-infected CNS (section 1.3.2). Cytosolic molecules involved in inflammatory or other innate immune responses may have potential roles not yet reported in prion infections. These could be therapeutic targets for prion diseases using immunomodulatory/anti-inflammatory drugs as interventions. Therefore, this study first focuses on the role of a well known proinflammatrory mediator, glatectin-3, in the disease development of murine scrapie 139A with the use of galaectin-3 knockout mice. In order to reveal the potential of the protein as a therapeutic target of the disease, the survival times, as well as, other histopathologies are investigated. Moreover, the possible role of galectin-3 to function as a PrP^{Sc} binding partner is also characterized. In the second part of the study, possible usage of simvastatin is explored in prion infections. Previous *in vitro* test reported beneficial effects of this relatively safe drug for cholesterol-lowering therapy in prion disorders (section 1.5.2). In this study, the *in vivo* effects of simvastatin in the infected CNS, particularly the immunomodulatory effects, are analyzed in wildtype mice inoculated with scrapie 139A.

3 Material and Methods

3.1 Material

3.1.1 Animals

C57BL/6 Mice	UC Davis, Sacramento/USA
Galectin-3 deficient (Galectin-$3^{-/-}$) Mice	UC Davis, Sacramento/USA

3.1.2 Scrapie Strain

Scrapie strain 139A	R.H. Kimberlin, Edinburgh/UK

3.1.3 Drug and Chemicals

Acetic Acid	Merck, Darmstadt
Acetone	Roth, Karlsruhe
Acrylamide Agarose	Life Technologies, San Fransisco/USA
Aqua Poly/Mount	Polyscience, Warrington/USA
Benzonase (Benzon Nuclease, purity 1)	Merck, Darmstadt
Brij 35 Solution	Merck, Darmstadt
Casein	Sigma, Deisenhofen
Chloroform	Roth, Karlsruhe
Citrate Acid Monophosphate	Merck, Darmstadt
Complete Mini (Protease inhibitor cocktail tablets)	Roche, Indianapolis/USA
Diethylpyrocarbonate (DEPC)	Fluka, Taufkirchen
Dimethylformamide (DMF)	Merck, Darmstadt
D.P.X. Neutral Mounting Medium	Sigma-Aldrich, Steinheim
Ethidium Bromide	Roth, Karlsruhe
Ethylendiamintetraacetate (EDTA)	Merck, Darmstadt
Ethanol	Roth, Karlsruhe
Formaldehyde	Merck, Darmstadt
Glycine	Serva, Heidelberg
Guanidinium Thiocyanate	Merck, Darmstadt
Hydrogen Peroxide (35%)	Roth, Karlsruhe
Immomix Solution	Bioline, Randolph/USA

Isopropanol	Roth, Karlsruhe
2-Mercaptoethanol	Sigma, Deisenhofen
Magnesium Chloride	Merck, Darmstadt
Methanol	Roth, Karlsruhe
Microscopy Aquatex®	Merck, Darmstadt
Paraffin	Roth, Karlsruhe
Sarkosyl	Serva, Heidelberg
Skimmed Milk Powder	TSI, Zeven
Sodium Acetate	Merck, Darmstadt
Sodium Chloride	Merck, Darmstadt
Sodium Dodecylsulfate (SDS)	Serva, Heidelberg
Sodium Phosphotungstate Dibasic Hydrate	Sigma, Deisenhofen
Tetramethylethylendiamine (TEMED)	Gibco BRL, Eggenstein
Tissue Freezing Medium	Jung, Nussloch
Tris	Sigma, Deisenhofen
Trizol	Invitrogen, Leek/NL
Tween 20	Serva, Heidelberg
Xylene	Roth, Karlsruhe
ZOCOR® (simvastatin)	MSD, Haar

3.1.4 Buffers and Solutions

Assay Buffer (pH 9.5)	100 mM Tris; 100 mM NaCl
Blotting Buffer	48 mM Tris; 38 mM Glycin; 0.037% SDS
Citrate Buffer (pH 6)	1.8 mM Citrate Acid; 8 mM Sodium Citrate
100bp DNA-ladder	Invitrogen, Leek/NL
10x DNAse Buffer	Ambion Huntington/UK
Fetal Bovine Serum (FBS)	Biochrom, Berlin
FBS/PBS (10%, 100 ml)	10 ml FBS; 90 ml PBS
Formaldehyde/PBS (4%)	0.4 g formaldehyde; 10 ml PBS
Haematoxylin Solution	Merck, Darmstadt
Laemmli Electrophoresis Buffer (10x)	250 mM Tris/HCL; 0.1% SDS; 1.92 M Glycine

MagicMark^{TM} XP (protein marker)	Invitrogen, Leek/NL
NTM (pH 9.5)	100 mM Tris-HCL; 100 mM NaCl; 50 mM $MgCl_2$
PBS (10x, pH 7.2)	137 mM NaCl; 2.7 mM KCl; 8 mM Na_2HPO_4; 1.5 mM KH_2PO_4
Proteinase K-Buffer	10 mM Tris; 100 mM NaCl; 0.5% Brij 35
Substrate Buffer	100 mM Tris; 100 mM NaCl; 5 mM $MgCl_2$
Stop Solution	20 mM EDTA/TBS
SYBR-Green Master Mix	Qiagen, Hilden
TBS (10x, pH 7.8)	50 mM Tris; 1 M NaCl
TBST	1x TBS with 0.05% (w/v) Tween20
Tris-Acetate-EDTA (TAE) Buffer (50x, 1 L)	2 mM Tris; 50 mM EDTA; 57.1 ml Acetic acid

3.1.5 Conjugates and Substrates for Immunohistochemistry and Immunoblot

2,3-Amino-9-Ethylcarbazol (AEC) + High Sensitivity Substrate	DakoCytomation, Carpinteria/USA
5-bromo-4-chloro-3-indolyl-phosphate (BCIP)	Sigma-Aldrich, Steinheim
CDP-Star	Tropix, Bedford/USA
3,3'Diaminobenzidine Tetrahydrochloride (DAB)	Sigma-Aldrich, Steinheim
Enhanced Chemiluminescence (ECL)	Amersham, Little Chalfont/UK
Nitro Blue Tetrazolium (NBT) Colour Solution	Sigma-Aldrich,Steinheim
Streptavidin Horseradish Peroxidase Conjugate	Amersham, Little Chalfont/UK

3.1.6 Antibodies

Table 1. Primary Antibodies

Antibody	Application/Dilution	Provider
Mouse anti-β-Actin (AC-15)	Western-Blot (1:500)	**Sigma, Munich**
Goat anti-mouse Galectin-3	Paraffin-section (1:400) Cryo-section (1:800) Western-Blot (1:1000)	**Drs. F.T. Liu & D. Hsu Sacramento/USA**
Rabbit anti-cow Glial Fibrillary Acidic Protein (GFAP)	Paraffin-section (1:1000) Cryo-section (1:2000)	**Dako, Glostrup/Denmark**
Rabbit anti-mouse Ionized Calcium Binding Adaptor molecule 1 protein (iba-1)	Paraffin-section (1:1000)	**Wako, Osaka/Japan**

Rabbit anti-rat LC-3	Western-Blot (1:1000)	**Prof. Y. Uchiyama Osaka/Japan**
Rat anti-mouse Mac-3 (LAMP-2)	Cryo-srction (1:100) Paraffin-section (1:50)	**Pharmingen San Jose/USA**
Rat anti-mouse I-A/I-E (MHC-II)	Cryo-section (1:10)	**Pharmingen San Jose/USA**
Mouse anti-Neuronal Nuclei (NeuN)	Cryo-section (1:200) Paraffin-section (1:200) Western-Blot (1:1000)	**Chemicon USA**
Mouse anti-PrP (4H11)	Western-Blot (1:5000)	**E. Kremmer Munich**
Mouse anti-PrP (6H4)	PET-Blot (1:10000)	**Prionics Zurich/Switzerland**

Table 2. Secondary Antibodies

Antibody	Dilution	Provider
Anti-Mouse Ig, alkaline phosphatase (AP)-conjugated	1:5000	**Dako, Glostrup/Denmark**
Anti-Mouse Ig, biotinylated	1:200	**Amersham, Little Chalfont/UK**
Anti-Mouse Ig, Cy3-conjugated	1:250	**Jackson ImmunoResearch, West Grove/USA**
Anti-Goat Ig, biotinylated	1:200	**Amersham, Little Chalfont, UK**
Anti-Goat Ig, Cy2-conjugated	1:250	**Jackson ImmunoResearch, West Grove/USA**
Anti-Rabbit Ig, AP-conjugated	1:5000	**Dako, Glostrup/Denmark**
Anti-Rabbit Ig, biotinyated	1:200	**Amersham, Little Chalfont/UK**
Anti-Rabbit Ig, Cy3-conjugated	1:250	**Jackson ImmunoResearch, West Grove/USA**
Anti-Rat IgG, biotinylated	1:200	**Amersham, Little Chalfont/UK**

3.1.7 Sodium Dodecyl Sulfate Polyacrylamide Gel (SDS-gel)

Table 3. Component of SDS-gel

Compositions	Separating Gel	Stacking Gel
Acrylamide	3.1ml	1.25ml
0.5M Tris/HCL, pH 6.8	1.25ml	1.25ml
20% SDS	50µl	50µl
Distilled water	4.3ml	3.07ml
TEMED	10µl	10µl
10% (w/v) APS	30µl	50µl

3.1.8 Commercial Kits

First-strand cDNA Synthesis Kit	Amersham, Braunschweig
RNeasy® Protect Mini Kit	Qiagen, Hilden

3.1.9 Enzymes

DNase I	Ambion, Huntingdon/UK
Proteinase K	Boehringer, Mannheim
Taq DNA Polymerase	Perkin Elmer, Langen
SYBR Green (50x)	Invitrogen, Leek/NL

3.1.10 Oligonucleotides

Primer for PCR

β-Actin	forward:	5'-CGC TCG TTG CCA ATA GTG AT-3'
	backward:	5'-AAG GCC AAC CGT GAA AAG AT-3'

Primer for Real-Time PCR

Atg3	forward:	5'-AGC TTT GCA GGC TTC CAC TA-3'
	backward:	5'-TGA TGG GGG ATG GGT AGA TA-3'
Atg5	forward:	5'-ATC AAC CGG AAA CTC ATG GA-3'
	backward:	5'-TTG GCT CTA TCC CGT GAA TC-3'
Beclin-1	forward:	5'-GGC CAA TAA GAT GGG TCT GA-3'
	backward:	5'-TGC ACA CAG TCC AGA AAA GC-3'
Lamp-2	forward:	5'-GAC TAC ATG GCG GTG GAA TA-3'
	backward:	5'-AGA GGG GCT GGT AGG TTG-3'
Glyceraldehyde-3-Phosphate Dehydrogenase (GAPDH)	forward:	5'-GAC CTC ACC ATC CCG CAT CT-3'
	backward:	5'-GCG GGA GTC GGC CAG TTA CC-3'

3.1.11 Apparatus and Devices

8 well plate (for PET-Blot)	Nunc, Roskilde/Denmark
Balance	Sartorius, Göttingen
Blotting paper	Schleicher & Schüll. Dassel
Blotting Chamber, Power Supply	Bio-Rad, Richmond/USA
Cover slip	Roth, Karlsruhe
Centrifuge	Heraeus, Hanau
Centrifuge tube (15ml/50ml)	TPP, Trasadingen/Switzerland
Dako-Pen	Dako, Carpinteria/USA
Development folder	Tropix, Bedford/UK
Embedding cassette	Roth, Karlsruhe
Electrophoresis power supply	Biotec-Fischer, Reiskirchen
Gas-liquid chromatography-flame ionization detector	Hewlett-Packard, Böblingen
Gas-liquid chromatography-mass spectrometry	Hewlett-Packard, Böblingen
Glassware (measuring cylinder, petri dish beaker)	Schott, Mainz
Histokinette processor	Leica Solms
Incubator	Heraeus, Hanau
Laser confocal microscope	Zeiss, Jena
Light microscope	Zeiss, Jena
Magnetic Immunostaining Trays	Cellpath, Newtown/UK
Magnetic stirrer	IKA, Staufen
Microwave oven	Sharp, Hamburg
Object slides tray	Roth, Karlsruhe
Optical cover for TaqMan-PCR	Applied Biosystems, Foster City/USA
Optical tube for TaqMan-PCR	Applied Biosystems, Foster City/USA
PCR reaction tube	SLG, Gauting
Pipette	Eppendorff, Hamburg Gilson,Columbus/USA
Pipette tip	Roth, Karlsruhe

Pipette tip with aerosol resistant filter	Biozym, Oldendorf SLG, Gauting
Polyvinylidene Difluoride (PVDF) membrane	Millipore, Bedford/UK
Reaction tube (1.5/2.0ml)	Neolab, Heidelberg
Real Time Cycler	Stratagene, La Jolla/USA
Shaker	Heidolph, Schwabach
Spectrophotometer	Pharmacia, Freiburg
SpeedVac Concentrator	Servant, Alberville/USA
Stereomicroscope	Leica, Solms
Table centrifuge	Heraeus, Hanau
Thermocycler	Biometra, Göttingen
Thermomixer	Eppendorf, Hamburg
Ultra-Turrax (homogenizer)	IKA, Staufen
Vortex-Mixer	Neolab, Heidelberg
Water Bath	Vogel, Oostsinge/NL

3.2 Methodology

3.2.1 Animal Experiments

3.2.1.1 Scrapie Infection of Galectin-3$^{-/-}$- and Wildtype-Mice

Scrapie strain 139A was used for the inoculation experiments in this study. 10% 139A-infected mouse brain homogenate was used as inoculum and was prepared from C57BL/6 mice brain tissue at the terminal stage of the disease. Galectin-3$^{-/-}$-mice on C57BL/6 background, together with the corresponding C57BL/6 wildtype (WT) controls were infected intracerebrally (i.c.) by injecting 20 µl of 10^{-4}-diluted inoculums into the fourth brain ventricle. In addition, intraperitoneal (i.p.) infection with two different infectious doses was performed by injecting 20 µl of undiluted or 10^{-2}-diluted inoculums to the peritoneal cavity of the animals. Negative controls (mock infections) were performed similarly with 10% brain homogenates prepared from uninfected, healthy C57BL/6 mice. All infections with the given dilution were performed on the same day and from the same brain homogenate aliquot to minimize variations among the infectious doses. All animals were kept under standardized conditions with regular 12-hour day-night period at 20˚C.

3.2.1.2 Simvastatin Treatment of Scrapie-infected WT Mice

C57BL/6 mice were used to examine the effect of simvastatin on scrapie-infected mouse brain tissues. In this study, i.c. infections were performed with two different dosages (10^{-3} or 10^{-4}). Mice were kept under the same conditions and inoculated in the same way as described in section 3.2.1.1. Simvastatin treatment commenced 100 days postinfection (dpi); hence at a time point when the infection of the central nervous system is already well established. The drug was administered orally as ingredient of the chow pellets for a daily dosage of 100 mg simvastatin per kg bodyweight.

3.2.1.3 Effects of Simvastatin on Cholesterol Metabolism

To determine the effect of simvastatin on normal brain cholesterol metabolism, the same treatment with the drug described in section 3.2.1.2 was performed on uninfected healthy C57BL/6 mice for 28 days. Cholesterol, its precursors lathosterol, lanosterol, and desmosterol, and its metabolites cholestanol and 24S-hydroxycholesterol (24S-OH-chol) were extracted from brains by chloroform/methanol and determined after derivation to the corresponding trimethylsilyl-ethers by gas chromatography-flame ionization detection (cholesterol) and gas chromatography-mass spectrometry (cholesterol precursors and metabolites) as described previously [192]. Dry weight of brain tissue was determined after drying them to constant weight overnight in a SpeedVac ultracentrifuge dryer.

3.2.1.4 Clinical Signs and Survival of Scrapie-infected Animals

In both galectin-3 knockout and simvastatin studies, animals were monitored twice per week for clinical signs of the disease, which included poor coat condition, hunched posture, hind leg paralysis, weight loss and behavioural changes (hyper-responsiveness to touch and nervousness). Galectin-$3^{-/-}$-mice and the corresponding WT controls were sacrificed at both, asymptomatic (125 days postinfection, dpi) and terminal stages of the disease. In the simvastatin treatment study, only mice at the terminal stage were examined. The terminal stage was defined as the development of the scrapie symptoms indicating that the animals would die, if not killed, within the next 72 hours. The survival rate in all groups was statistically analysed by the unpaired *t*-test.

3.2.1.5 Sample Collection and Fixation

Animals in both studies were sacrificed and brains were collected. The brain samples were divided sagittally into two brain hemispheres. One half of it was fixed in 4% PBS-formaldehyde for 24 hours before subjected to paraffin block preparation. The other half was frozen immediately in liquid nitrogen without any fixation processes. A part of some frozen samples were embedded in cryomolds with tissue freezing medium and then stored at -70 ˚C for later cryo-section preparation. The rest was stored at the same temperature until used for brain homogenate preparation or RNA extraction.

3.2.2 Histology and Immunohistochemistry

3.2.2.1 Preparation of Paraffin- and Cryo- Sections

The brain samples fixed in 4% PBS-formaldehyde (section 3.2.1.5) were dehydrated and embedded in histological paraffin blocks at 60˚C on the second day as described below:

Ethanol 70%	**12 hours**
Ethanol 70%	**40 minutes**
Ethanol 80%	**40 minutes**
Ethanol 90%	**40 minutes**
Ethanol absolute	**2 x 40 minutes**
Ethanol 50%/Xylene 50%	**2 x 30 minutes**
Xylene	**2 x 30 minutes**
Paraffin	**3 x 25 minutes**

6 μm sagittal paraffin sections were cut from the embedded samples using a microtome. The sections were stretched in water bath at 50˚C before being mounted on object slides. The mounted samples were dried overnight in an incubator at 37˚C before immunohistochemical labelling procedure. 8 μm sagittal cryo-sections were prepared from samples embedded in cryomolds (section 3.2.1.5) by cryotome at -20˚C. The sections were mounted on object slides and fixed in acetone at -20˚C for 10 minutes. The mounted samples were then dried at room temperature (RT) for one hour and then stored in -20˚C.

3.2.2.2 Immunohistochemical Labelling

Avidin-Biotin-Complex (ABC) method was employed to increase the intensity of the signals from the recognized antigen by the corresponding primary antibody. The intensification is a result of the strong affinity of the glycoproteins Avidin/Streptavidin with Vitamin Biotin. The first step involved the recognition of specific antigen by a suitable non-conjugated primary antibody. It was then identified by the corresponding biotinlynated secondary antibody.

Afterwards, Avidin/Streptavidin conjugated peroxidase was allowed to bind to the biotin linked secondary antibody. Finally, substrate for peroxidase, for example AEC or DAB, was added to give the corresponding colouration. In addition, secondary antibodies linked with fluorophores, such as Cy2 and Cy3, were also used.

3.2.2.3 Immunohistochemical Labelling of Activated Glial Cells

Labelling was performed on paraffin sections unless specified otherwise. Activated astrocytes in the scrapie-infected brain tissue were identified using anti-GFAP antibody. Microglia were recognized by protein markers iba-1, LAMP-2, galectin-3 and MHC-II (cryo-sections). The dilution for these markers and the corresponding biotinylated secondary antibodies are listed in section 3.1.6. Standard protocol for the staining procedures is described below:

Xylene }	***(Not applicable to cryo-sections***	**2 X 5 minutes**
Acetone }	***staining)***	**2 X 5 minutes**
PBS }		**2 X 5 minutes**
3% H_2O_2 /Methanol	***(Blocking of endogenous peroxidase)***	**30 minutes**
PBS		**2 X 5 minutes**
Blocking with 10% FCS/PBS		**30 minutes**
Glial cells recognizing antibody (in 10% FCS/PBS)		**1 hour (37˚C)/overnight (4˚C)**
PBS		**2 X 5 minutes**
Corresponding secondary antibody (in 10% FCS/PBS)		**1 hour, (RT)**
PBS		**2 X 5 minutes**
Streptavidin peroxidase complex (1:200 in 10% FCS/PBS)		**45 minutes (37˚C)**
PBS		**5 minutes**
Colouration with AEC or DAB		**-**

AEC coloured slides were counterstained with haematoxylin and then mounted with Aquatex. Samples incubated with DAB were first subjected to dehydration with alcohol (50%, 70%, 80%, 99%) and absolute xylene before being counterstained and mounted with Paramount. The mounted samples were dried overnight and then decontaminated with 2% sodium hydroxide before being analysed.

3.2.2.4 Fluorescent Double-Labelling

Paraffin sections were double-labelled by antibodies identifying GFAP, iba-1, galectin-3 and NeuN. The fluorescence was generated by Cy2 and Cy3 linked to corresponding secondary antibody. Dilutions for the different antibodies are listed in section 3.1.7 and the protocol is shown below:

Xylene	**2 x 5 minutes**
Acetone	**2 x 5 minutes**
PBS	**2 x 5 minutes**
Blocking with 10% FCS/PBS	**30 minutes**
Anti-glial cells/neurons antibody (in 10% FCS/PBS)	**1 hour (37˚C)**
PBS	**2 x 5 minutes**
Corresponding Cy2/Cy3-conjugated secondary antibody (in 10% FCS/PBS)	**1 hour**
PBS	**2 x 5 minutes**

Samples were mounted immediately with Aqua Poly/Mount and were decontaminated in the same way as mentioned in section 3.2.2.3.

3.2.2.5 Preparation of Paraffin-Embedded Tissue Blot (PET-Blot)

The profiles of PrP^{Sc} deposition were analysed using the PET-Blot technique in the galectin-$3^{-/-}$-study. This is a method with high sensitivity enabling the detection of very low levels of PrP^{Sc}. Additionally, it preserves the morphology of the brain sample after proteinase K (PK) digestion, therefore provides a satisfactory anatomical resolution when compared to other histoblot techniques. 8µm sagittal sections of formalin-fixed brain tissue (section 3.2.1.5) were prepared by microtome. Samples were mounted on nitrocellulose membranes and dried overnight at 60˚C. The procedure for further immunohistochemisty is shown below:

Xylene	**2 x 5 minutes**
95% Isopropanol	**5 minutes**
80% Isopropanol	**5 minutes**
70% Isopropanol	**5 minutes**
50% Isopropanol	**5 minutes**
0.1% Tween/double distilled water	**2 x short washing**
The membrane was dried	**10 minutes (60˚C)**
TBST	**20 minutes**
PK digestion	**2 hours (55˚C)**
TBST	**3 x 10 minutes**
Denaturation of protein with 3M Guanidiniumthioisocyanate at RT	**10 minutes**
TBST	**3 x 10 minutes**
Blocking with 0.2% Casein/TBST	**30 minutes**
Anti-6H4 in 0.2% Casein/TBST	**Overnight (4˚C)**
TBST	**3 x 10 minutes**
AP-conjugated Anti-Mouse-IgG (1:100 in 10% FCS/PBS), RT	**1 hour**
TBST	**5 x 10 minutes**
Pre-incubation with NTM	**2 x 10 minutes**
Colour development with NBT/BCIP	**10 minutes**
Stop of colour development	**5 minutes**
Distilled water	**3 x short washing**
The membrane was dried	**1 hour (60˚C) .**

3.2.2.6 Analysis of Immunohistology

A semi-quantitative valuation system was used to investigate the immunohistology of the infected brains. Sagittal brain sections were divided and observed in seven different anatomical regions (diagram 2) namely, olfactory lobe (Olf), cortex (Cort), hippocampus (Hipp), striatum (Stri), thalamus (Th), cerebellum (Cereb) and medulla (Med) according to the mouse brain atlas (Franklin & Paxinos, 2002). In each region, AEC/DAB-stained samples were analysed under a light microscope in the magnification of 400-fold. On the other hand, the intensity of the stained PrP^{Sc} on PET-Blot-sections was analysed by a stereomicroscope. The variations or differences in immunohistology of microgliosis, astrocytosis and PrP^{Sc} accumulation between samples were assessed. All analyses were carried out using anonymous slides prepared from at least three different and independent animals. In addition, all samples were analysed by two independent investigators. Galectin-3-expressing cell type was analysed by fluorescence double staining using confocal microscopy.

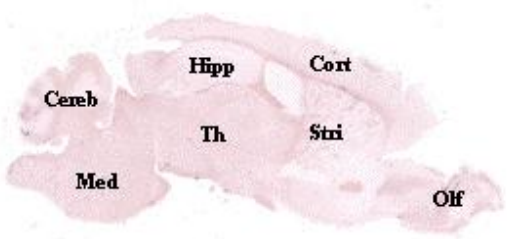

Diagram 1. Sagittal section of mouse brain showing the analysed anatomical regions

3.2.3 Protein Analysis by Western-Blot

3.2.3.1 Tissue preparation

The Western-Blot analysis is an immunological method for detecting proteins collected from cell cultures or whole tissue samples. This method was used for analyzing the PrP^{Sc} accumulation in scrapie-infected CNS. 10% mouse brain homogenate (3.2.1.5) was used for this study. 10 g of brain tissue was first mechanically broken down by homogenization and sonication in 100 ml PBS with 0.5% Triton X-100 and protease inhibitor tablet. Detergent in the buffer helps solubilize protein samples while protease inhibitor prevents digestions of the samples by its own enzymes. Samples for PrP^{Sc} accumulation analysis were further incubated and digested with PK (50 µg/ml) at 37˚C for one hour. The PK treatment helped remove PrP^{c} from the treated-samples (+PK-sample) which would otherwise be recognized together with

PrP^{Sc} by the anti-prion protein antibodies. The corresponding control (-PK-sample) was prepared by incubating the samples at 37˚C in the homogenization buffer for one hour. All samples were finally stored at -20˚C until used.

3.2.3.2 SDS Polyacrylamide Gel Electrophoresis (SDS-PAGE)

Proteins were separated according to their molecular weight by gel electrophoresis using polyacrylamide gels containing SDS. Proteins were first denatured by a strong reducing agent, 2-mercaptoethanol, to remove secondary and tertiary structures such as S-S disulfide bonds. The SDS-PAGE maintains polypeptides in the denatured negatively charged state. The concentration of the separating gel is 12.5% of and the stacking gel is 5% of acrylamide, respectively (section 3.1.7). 20 µl of protein samples prepared in section 3.2.3.1 and the corresponding weight markers were loaded onto the SDS-gels in a vertical electrophoresis chamber running at 200V in electrophoresis buffer.

3.2.3.3 Transfer of Proteins to PVDF Membrane and Chemiluminescent Detection

Separated proteins in SDS-gel were made accessible to antibody detection through their transfer onto a 0.45 mm thick PVDF membrane by electroblotting. The gel and membrane were first activated with absolute methanol and then placed between two filter papers moistened by 20% (v/v) methanol/blotting buffer. Finally, the whole cassette was placed in a blotting chamber and blotted for 20 minutes at 200 V (per gel). To reduce non-specific interactions between antibodies and the membrane, 3% dry milk with trace amount of detergent, Tween 20, was used as blocking reagent. Targeted proteins were probed overnight at 4˚C with antibodies listed below:

Protein	Antibody
Actin	Anti-actin (AC-15)
LC-3	Anti-LC-3
Prion protein	Anti-4H11

The membrane was then washed with TBST and 3% milk/TBST before incubation with the corresponding AP-conjugated secondary antibody at RT for 90 minutes. After that, it was washed again with TBST and followed by blocking with 3% milk/TBST for 1 hour. The membrane was then pre-incubated with Assay buffer for 5 minutes two times. Finally, the

membrane was incubated with 5ml of CDP-Star (with a concentration of 1:100 in the assay buffer), and luminescence was detected by photographic film. If necessary, the results were analysed densitometrically.

3.2.3.4 Sodium Phosphotungstic Acid (NaPTA) Precipitation

In addition to examining the protein expression profile of scrapie-infected CNS, Western-Blot was employed for demonstrating the interactions of PrP^{Sc} with other cellular proteins. The collected brain tissue (section 3.2.1.5) was purified by NaPTA precipitation prior to investigation. This method selectively precipitates PrP^{Sc} from a pool of proteins using NaPTA at neutral pH in the presence of Mg^{2+}. NaPTA generates complexes with oligomers/polymers of infectious PrP^{Sc} and PrP^{27-30} but not with the normal PrP^{c} protein (diagram 3).

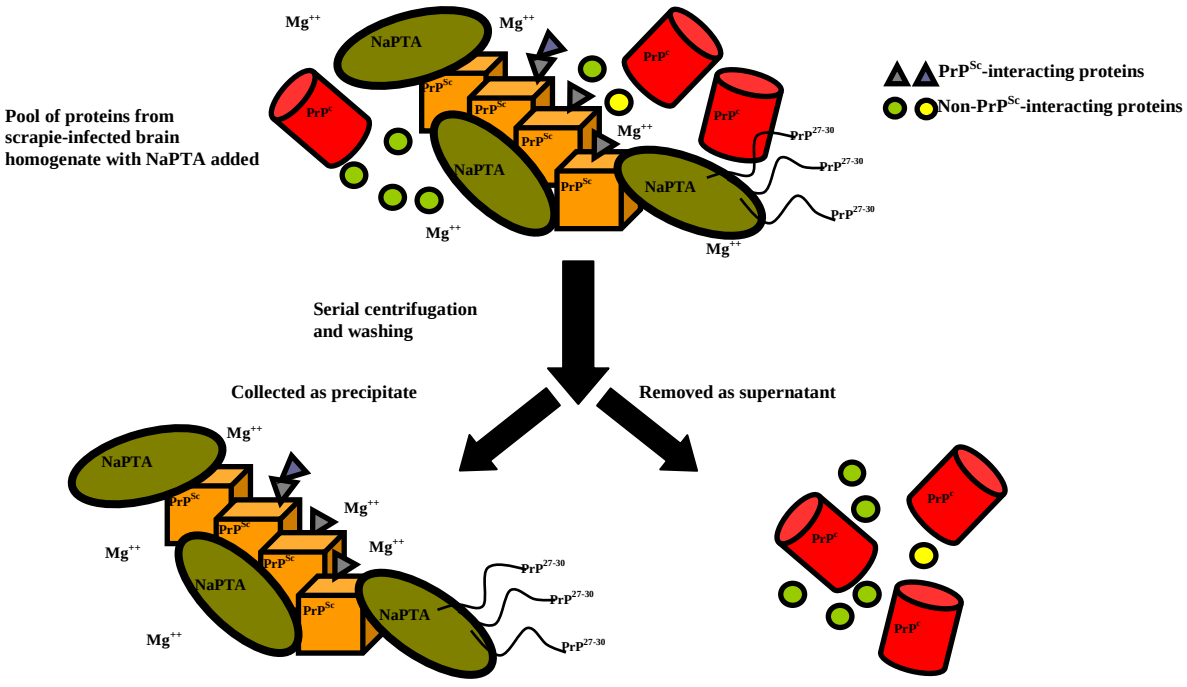

Diagram 2. General principle of PTA precipitation of PrP^{Sc} protein

The resultant purified precipitate consists of significantly PrP^{Sc} and only a trace amount of other PrP^{Sc}-interacting proteins [54]. Briefly, 10% brain homogenates were prepared in PBS without calcium and magnesium salts followed by centrifugation at 80 g for 1 minute. Supernatant was collected and diluted with 4% (w/v) sarkosyl/PBS (pH 7.4) and incubated at 37°C for 10 minutes. Benzonase/$MgCl_2$ with a final concentration of 1 mmol/l was then added to the samples at 37°C for 10 minutes. Sodium phosphotungstic acid with final concentration of 0.3% (w/v) was added. The samples were further incubated for 30 minutes at 37°C and followed by centrifugation at 15800 g. Supernatant was removed and the pellet was resuspended in 0.1% (w/v) sarkosyl/PBS (pH 7.4) and 250mmol EDTA (pH 8). The samples were centrifuged at 15800 g and finally resuspended in 0.1% (w/v) sarkosyl/PBS (pH 7.4) as stock.

PTA precipitate and total brain homogenates of terminally scrapie-infected and mock-infected mouse brains were examined and both materials were adjusted to the identical concentration (0.02 brain unit) prior to the blotting experiments. Interactions between PrP^{Sc} and other cellular proteins were detected by Western-Blot using antibodies listed below:

Protein	Antibody
Galectin-3	Anti-Galectin-3
Lamp-1	Anti-Lamp-1
Neuronal nucleic	Anti-NeuN
Prion protein	4H11

3.2.4 Molecular Biology

3.2.4.1 Precaution of RNA Work

Since isolated RNA is easily destroyed by RNase, RNase-free equipments are important for RNA work. Pipettes reserved for RNA works and RNase-free pipette tips with filter were used. Commercially available RNase-free reagents and plastic ware were used. For RNase inactivation, deionized water was incubated overnight with 0.1% DEPC at 37˚C. For DEPC inactivation the DEPC-treated water was autoclaved (DEPC-H_2O). Glassware was baked for 20 hours at 200˚C for RNase inactivation. If possible all procedures were performed on ice.

3.2.4.2 Isolation of Total RNA from Mouse Brain Tissue

The brain samples stored at -70˚C (section 3.2.1.5) were homogenized with a Ultra-Turrax in a 50ml centrifuge tube with 1ml Trizol/100mg tissue. The foam developed after homogenization was settled by centrifugation at 1435g (4˚C) for 3 minutes. The supernatant was transferred to an eppendorf tube and centrifuged at 12000g (4˚C) for 10 minutes. Afterwards, supernatant was collected and incubated at RT for 5 minutes. 0.2ml of choloform was added, followed immediately by 15 seconds of strong shaking and an incubation of 3 minutes at RT. For phase separation the sample was subjected to another centrifugation for 15 minutes at 12000g (4˚C) and the RNA-containing supernatant was collected again. 0.5ml of isopropanol was added to the collected supernatant and followed immediately by strong shaking for 15 seconds. The supernatant was removed and the RNA containing pellet was washed with 1ml of ice cold 70% ethanol followed by a final centrifugation step at 7500g (4˚C) for 5 minutes. The RNA containing pellet was incubated at 37˚C for 10 minutes to remove the alcohol and was resuspended in 100µl of DEPC-H_2O. Concentration of the collected total RNA was assessed by measuring their absorbance at the wavelength 260nm (A260) using a spectrophotometer. The isolated RNA was stored at -70˚C until used.

3.2.4.3 Removal of Genomic DNA from Total RNA

Any genomic DNA contamination present in the total RNA may interfere with the results of quantitative real-time PCR. In order to remove this contamination, 20µg of total RNA was incubated with 3µl of DNase I and 3µl of DNase buffer in a final volume of 30µl at 37˚C for 45 minutes. RNeasy Protect Mini Kit was used for removal of enzymes and other contaminants according to the manufacturer's guide.

3.2.4.4 cDNA Synthesis

cDNA for gene expression analysis was synthesised from total RNA using reverse transcriptase polymerase chain reaction (RT-PCR). First-strand cDNA Synthesis Kit was employed for the process. The purified total RNA (section 3.2.4.4) was first incubated for 5 minutes at 65˚C to denature the secondary structure of the RNA. The sample was incubated into ice cold water immediately after this step. 1µl each of random hexamer primer [$pd(N)_6$] and the poly(A)-tail specific oligo (dT) primer [$(dT)_{18}$] was then added. Together with 5µl of bulk first strand

reaction mix and 1µl of DTT, the reaction mixture was further incubated at 37˚C for 1 hour. Negative control was prepared for each sample by replacing the bulk first strand reaction mix with distilled water to confirm absence of genomic DNA in later quantitative real-time PCR. The synthesised cDNA was stored at -20˚C until used.

3.2.4.5 Control Polymerase Chain Reaction (PCR) with β-Actin

To ensure the quality of the synthesised cDNA (section 3.2.4.5), PCR of the samples with primers for the housekeeping gene β-actin was performed. Each PCR reaction mixture contains 12.5µl of 2X PCR mix (with 25mM $MgCl_2$ and 2.5mM dNTP), 1µl of each primer (β-actin forward and β-actin backward, 10µM each) and 0.5µl of the cDNA sample. The final reaction volume was made up to 50µl with PCR water. PCR was performed in a Thermocycler with the condition listed below:

Control PCR with β-Actin

Activation of the DNA polymerase	10 minutes	95˚C	
Denaturation of the cDNA	30 seconds	95˚C	X 35 Cycles
Annealing (ideal temperature for β-actin primers)	30 seconds	62˚C	
Elongation	1 minute	72˚C	
Final elongation step	Optional	72˚	

The PCR products were analysed using gel electrophoresis with the gel consisting of 1% agarose in 1X TAE with 0.5µg/ml of ethidium bromide (EB). Electrophoresis was performed in an electrophoretic chamber at 100V with 1X TAE buffer as running buffer. EB in the gel intercalated between DNA base pairs of the target sequence. The EB-tagged sequences appeared as fluorescent bands on the agarose gel when exposed to UV light.

3.2.4.6 Quantitative Real-Time PCR

Differences in gene expression of scrapie-infected galectin-3$^{-/-}$- and WT- mice, as well as uninfected controls were analysed by quantitative real-time PCR using cDNA prepared from these samples (section 3.2.4.4). The method allows comparison of gene expression between samples with differences down to two-fold change. The fluorescence dye SYBR Green was used as reporter for the amplification reaction which binds to double-stranded DNA and enables direct analysis of the relative amount of target sequence. Fluorescence signal from the SYBR-Green-bound template was measured at the end of every PCR cycle and was presented in the amplification plot as shown in diagram 4.

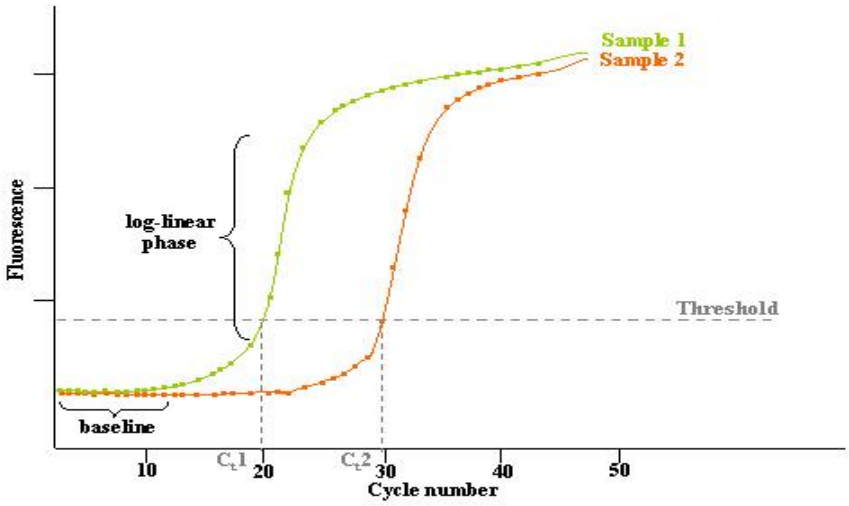

Diagram 3. Amplification plot of quantitative real-time PCR showing increases in fluorescence from samples in response to the increases in number of reaction cycles

Each tested sample was represented by an amplification curve in the plot showing the increased amount of sample in each PCR cycle. Quantification was performed by setting a threshold line within the log-linear phase of the amplification to indicate when the amount of template began significantly to increase. The cycle number at which the sample reaches this level is called the Cycle threshold (C_t). The C_t value is correlated to the initial amount of the target template: the higher the starting copy number of the template, the sooner the significant fluorescence increment level is reached. The collected results (corresponding C_t value of samples and control: $C_{t[\text{target gene of samples/control}]}$) were analysed by $\Delta\Delta C_t$ method to determine the expression profile of the target gene. To compensate variations in amount of input cDNA of samples and corresponding control, an endogenous house-keeping gene, glyceraldehyde-3-phosphate

dehydrogenase (GAPDH), was quantified ($C_{t[\text{GAPDH of samples/control}]}$) and results were normalized to these values as described in step 1 of table 4. Finally, $\Delta\Delta C_t$ value between sample and control was calculated using these normalized values (table 4, step 2) and the relative expression of the target gene was determined from the $\Delta\Delta C_t$ (table 4, step 3).

Table 4. Calculation of the $\Delta\Delta C_t$ method

Step 1	Normalized $\Delta C_{t[\text{target gene of samples/control}]} = C_{t[\text{target gene of samples/contro}]} - C_{t[\text{GAPDH of samples/control}]}$
Step 2	$\Delta\Delta Ct$ = Normalized $\Delta Ct_{[\text{target gene of samples}]}$ – Normalized $\Delta Ct_{[\text{target gene of control}]}$
Step 3	Gene expression level = $2^{(\Delta\Delta Ct)}$

The final reaction volume of SYBR Green real-time PCR was 12.5µL (Table 5). The amplification reaction was performed using a real-time PCR cycler with running program as described in section 3.2.4.5. For each cDNA sample (section 3.2.4.4) a 10-fold dilution was performed using tRNA-water (1:1000) and three reactions were carried out. In addition, one reaction for the corresponding negative control (3.2.4.4) was prepared to serve as a control for DNA contamination.

Table 5. Pipetting scheme for SYBR Green real-time PCR

Immomix Sol.	6.25µL
MgCl2 (50mM)	0,375µL
SYBR Green (50X)	0,25µL
Primer a (10µM)	0,36µL
Primer b (10µM)	0,36µL
cDNA (10X diluted)	2µL
PCR-water	Up to 12.5µL

4 Results

4.1 Role of Galectin-3 in Scrapie Infection

cDNA expression of galectin-3 is highly upregulated during scrapie infections [193]. Therefore, the protein expression profile of galectin-3 and its expressing cells were analysed. To investigate the role of galectin-3 in scrapie pathogenesis, galectin-$3^{-/-}$-mice were infected and compared to WT controls. Furthermore, interaction between galectin-3 and PrP^{Sc} was also demonstrated.

4.1.1 Expression Profile of Galectin-3 After Scrapie Infection

To determine the expression profile of galectin-3 in the CNS after scrapie infection, galectin-3 protein expression in infected WT mice with background C57BL/6 was immunohistochemically analysed at 125 dpi and the terminal stage of disease. As shown in figure 1B, galectin-3 was expressed early after scrapie infection. Pronounced galectin-3 expression was found in the infected CNS at the terminal stage of the disease (figure 1C). No galectin-3 expression was found in the mock-infected healthy CNS (figure 1A).

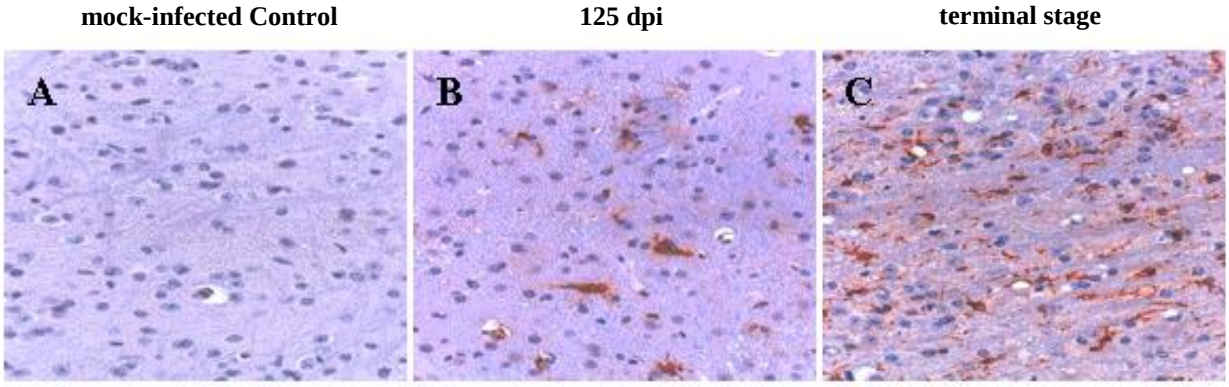

Figure 1. Galectin-3 expression of scrapie-infected mouse CNS. Medulla oblongata, 400-fold. (A) mock-infected control, (B) 125dpi and (C) terminal stage of disease.

4.1.2 Galectin-3-expressing Cells in Scrapie-infected CNS

Given that numerous cell types in the CNS and PNS have been shown to express galectin-3, the galectin-3-expresssing cell type in scrapie-infected mouse brains was characterized by double labelling and confocal microscopy. Astrocytes, neurons and microglia cells from scrapie-infected CNS were examined at the terminal stage using GFAP, NeuN and iba-1, respectively, as the corresponding protein markers. GFAP, NeuN and iba-1 are indicated by the red fluorescence (figure 2B, 2E and 2H) while galectin-3 is represented by the green fluorescence (figure 2A, 2D and 2G). Galectin-3 was not expressed in astrocytes as indicated in figure 2C which is the merged image of figure 2A (galectin-3) and 2B (GFAP). It was not found in neurons either as shown in figure 2F, the merged image of figure 2D (galectin-3) and 2E (NeuN). However, galectin-3 was co-expressed with iba-1 expressing cells indicated by figure 2I which is the merged image of figure 2G (galectin-3) and 2H (iba-1). These results indicate that galectin-3 is expressed by microglia cells

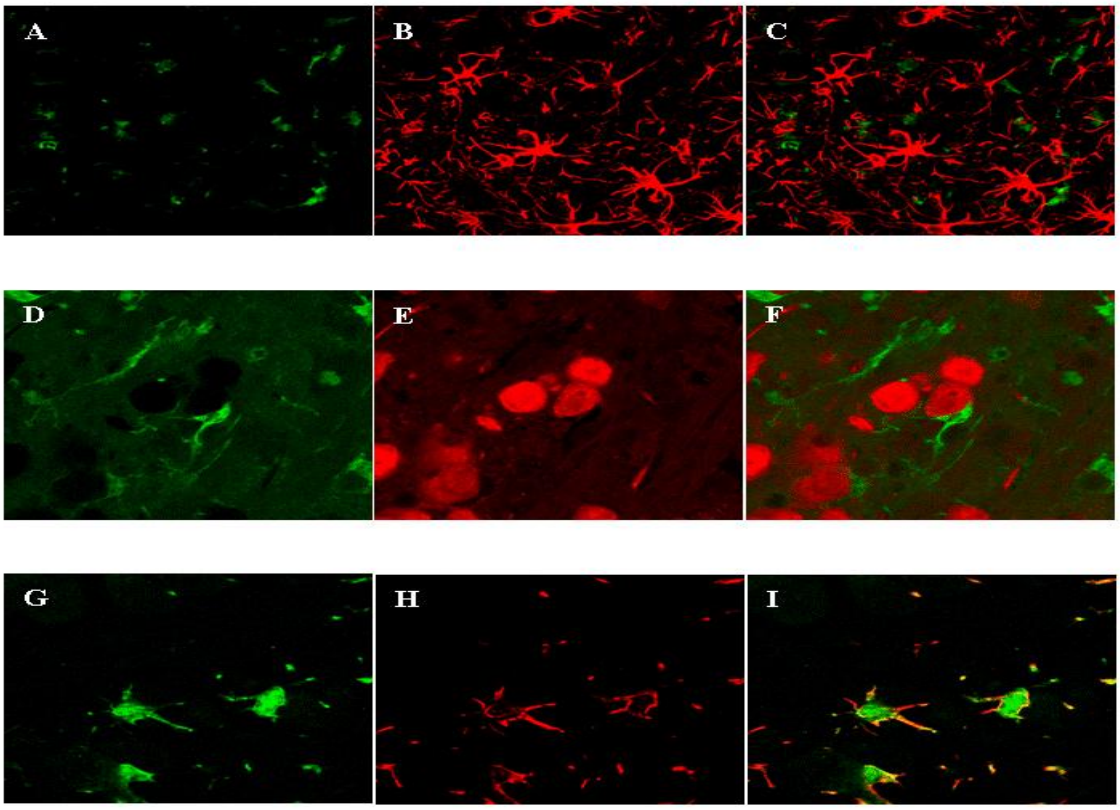

Figure 2. Confocal images of the double labelling of scrapie infected mouse CNS. (A), (D) & (G): galectin-3 staining, (B): GFAP staining for activated astrocyte, (E): NeuN staining for neurons, (H): iba-1 staining for microglia. (C): merged image of (A) & (B), (F): merged image of (D) & (E), (I): merged image of (G) & (H).

4.1.3 Prolonged Survival Times of Scrapie Infected Galectin-3$^{-/-}$-Mice

In order to study the role of galectin-3 in scrapie pathogenesis, galectin-3$^{-/-}$- and WT- mice were challenged intracerebrally or intraperitoneally with different dosages of scrapie-infected brain homogenates (section 3.2.1.1). Compared to the similarly infected WT mice the survival time of galectin-3$^{-/-}$-mice was significantly prolonged ($p<0.01$) upon i.p. and i.c. infection. I.p.-infected galectin-3$^{-/-}$-mice survived up to 22 days longer than the WT controls. Following i.c. infection, survival times of the knockout mice were prolonged in average by 16 days (table 6).

Table 6. The survival times of galectin-3$^{-/-}$-mice and WT controls upon different modes of infections with inoculums (dpi)

Dilution of 10% brain homogenates and route of infection (i.p. or i.c.)	Galectin-3$^{-/-}$-mice survival times (dpi)	WT control mice survival times (dpi)
Undiluted (i.p.)	Mean 223±10, n=8* (202, 216, 217, 226, 227, 227, 233, 234)	Mean 201±13, n=9 (171, 195, 198, 206, 209, 209, 209. 209, 209)
10^{-2} (i.p.)	Mean 233±11, n=10* (221, 221, 227,228, 231, 233, 234, 234, 240, 259)	Mean 214±6, n=10 (207, 207, 210, 210, 214, 214, 217, 219, 221, 226)
10^{-4} (i.c.)	Mean 210±13, n=8* (192, 202, 203, 206, 209, 209, 227, 231)	Mean 194±9, n=10 (175, 188, 188, 191, 192, 195, 198, 198, 204, 206)

*** $p< 0.01$ versus control group**

4.1.4 PrP^{Sc} Accumulation

PrP^{Sc} accumulation and propagation are of a central importance in prion infections. To examine the scrapie-infected animals in more detail, the accumulation of misfolded PK-resistant PrP^{Sc} in i.c. infected WT controls and galectin-$3^{-/-}$-mice were studied using PET-Blot analysis. As shown in figure 3, no significant differences in the PrP^{Sc} accumulation in scrapie-infected brains could be found in galectin-$3^{-/-}$-mice compared to WT controls, neither at the asymptomatic stage nor the terminal stage of disease. Distribution and intensity of PrP^{Sc} staining was approximately identical between knockout- and WT- mice.

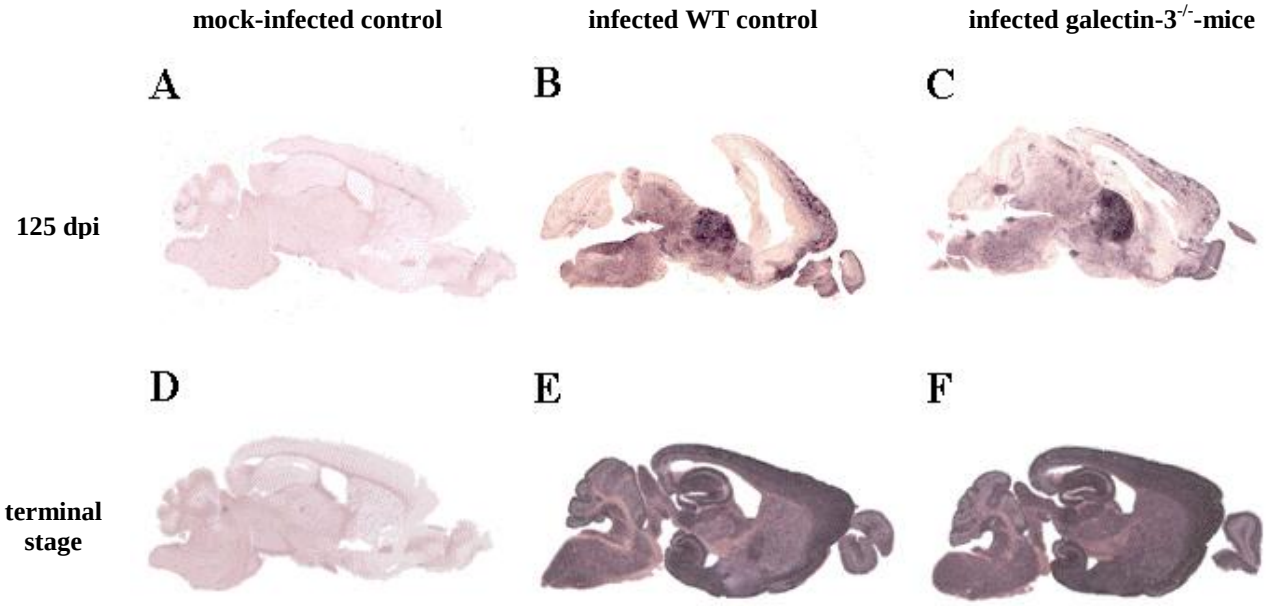

Figure 3. PET blot analysis of PrP^{Sc} accumulation in the galectin-$3^{-/-}$-mice and the WT controls. (A) & (D): mock-infected mice, (B) & (E): scrapie-infected WT controls and (C) & (F): scrapie-infected galectin-$3^{-/-}$-mice. (A) to (C): 125 dpi and (D) to (F): terminal stage of disease.

4.1.5 Astrocytosis

Astrocytes have been reported as active participants in prion pathogenesis [106, 194]. The activation and proliferation of astrocytes were examined with the help of immunohistochemistry using the protein marker GFAP. Upregulated expression of the protein was found in all of the examined brain regions as mentioned in section 3.2.2.6 after scrapie infection. Only a mild expression of the protein could be detected in uninfected and healthy brain tissues as shown in figure 4A and D. However, as demonstrated in figure 4B and C, no significant differences could be found between galectin-3$^{-/-}$-mice and WT controls at 125 dpi. Similar results were observed at the terminal stage of the disease (figure 4E and F).

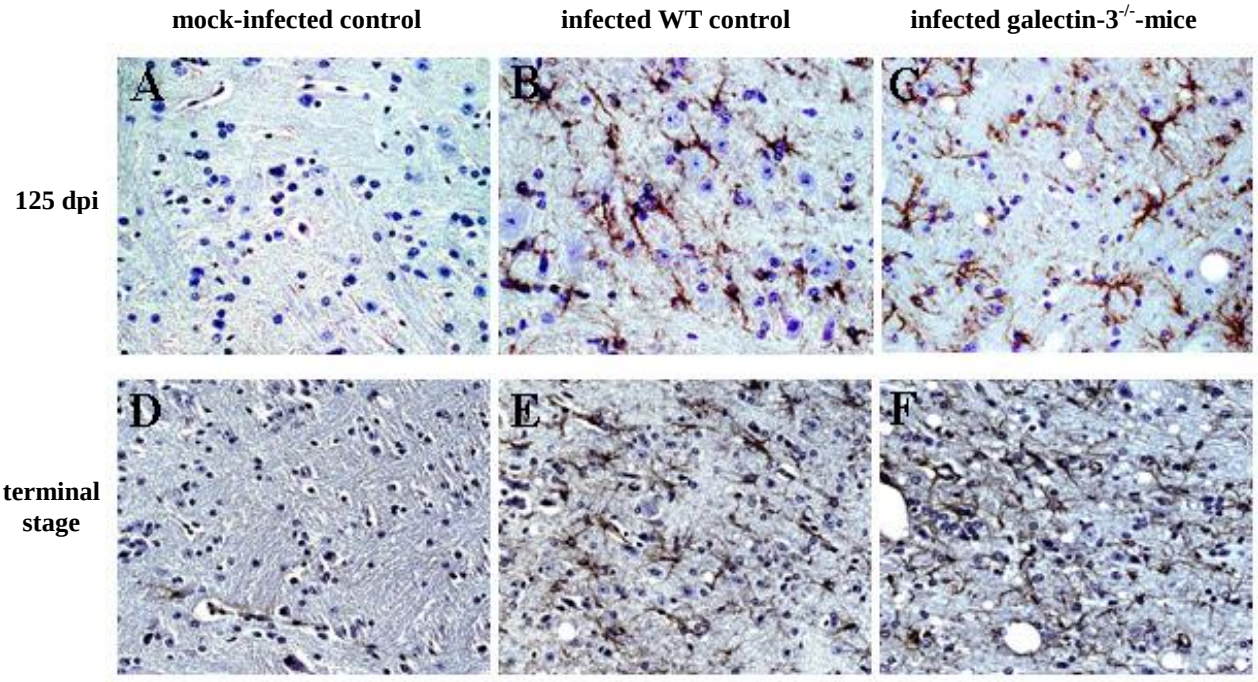

Figure 4. Immunohistochemical staining of GFAP-positive activated astrocytes in the galectin-3$^{-/-}$-mice and the WT controls. (A) & (D): mock-infected mice, (B) & (E): scrapie-infected WT controls and (C) & (F): scrapie-infected galectin-3$^{-/-}$-mice. (A) to (C): 125 dpi and (D) to (F): terminal stage of disease.

4.1.6 Microgliosis

In the scrapie model studied here galectin-3 is expressed by activated by microglia (section 4.1.2). The scrapie-induced microgliosis was further analysed by examining immunohistologically the expression of Iba-1, a marker for resting, as well we, activated microglial cells. As expected, basal expression of Iba-1 was found in the mock-infected controls at both stages of the disease in all observed brain regions (figure 5A and D). In scrapie-infected tissue, Iba-1 expression was upregulated at the early stage of infection (figure 5B and C) and became more profound at the terminal stage as shown in figure 5E and F. Similar to the GFAP expression (section 4.1.5), no significant differences of Iba-1 expression could be found between galectin-$3^{-/-}$-mice and WT controls at both stages of disease. In addition, the morphology of Iba-1 positive cells in scrapie-infected knockout- and WT- animals was similar. They appeared as typical activated microglial cells with thick and short processes extending from a large cell body (figure 5B to C and E to F).

The immunohistochemical analysis of the microgliosis was then extended to another typical microglia marker, Mac-3, which is also a binding partner of galectin-3 [159]. It is also called lysosomal associated membrane protein-2 (LAMP-2) and is a lysosomal activation marker protein [195]. LAMP-2 together with another highly glycosylated protein, lysosomal associated membrane protein-1 (LAMP-1), contribute to approximately 50% of all proteins of the lysosomal membrane [196]. Neither WT controls nor galectin-$3^{-/-}$-mice expressed detectable levels of LAMP-2 at the asymptomatic stage of the disease as demonstrated in figure 6. However, profound upregulation of the protein at the terminal stage was demonstrated in medulla oblongata, striatum and cerebellum after infection in WT controls (figure 7G to I). Intriguingly, LAMP-2 expression was undetectable in galectin-$3^{-/-}$-mice even at the terminal stage of disease and appeared similar to the mock-infected animals (figure 7D to F). Taken together, galectin-3 appears to be involved in the regulation of LAMP-2 expression.

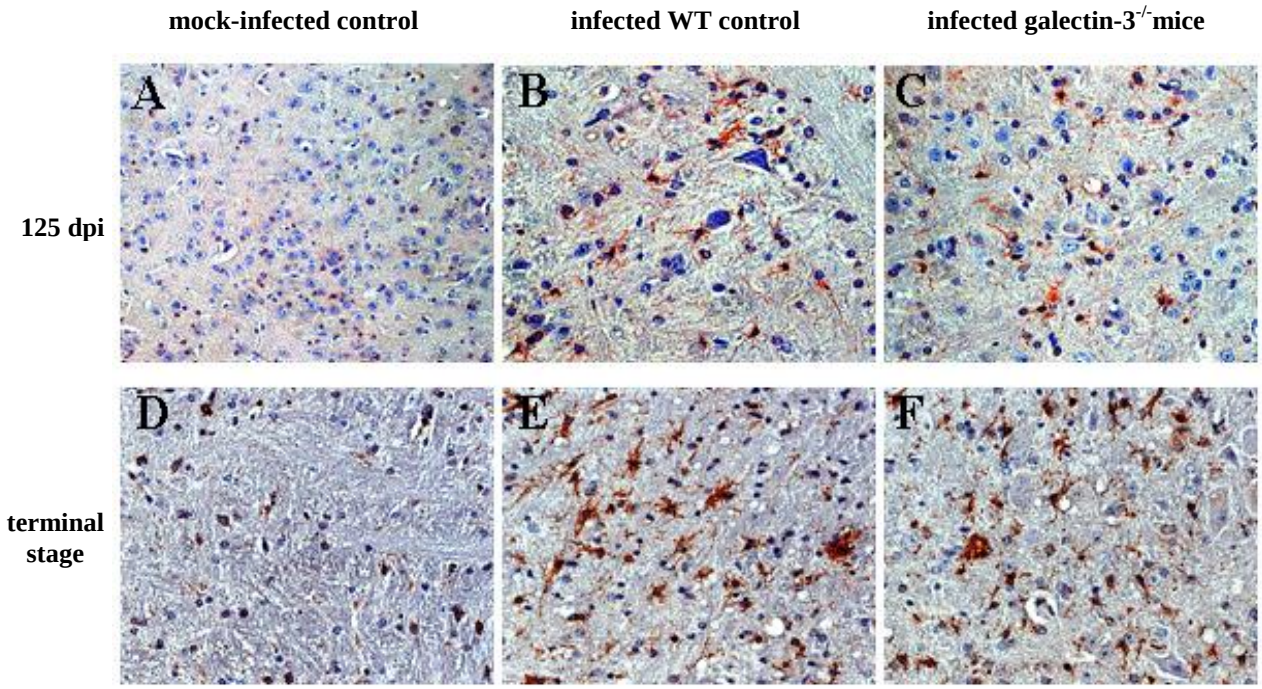

Figure 5. Immunohistochemical staining of Iba-1-positive microglia; in the galectin-3$^{-/-}$-mice and the WT controls. (A) & (D): mock-infected mice, (B) & (E): scrapie-infected WT controls and (C) & (F): scrapie-infected galectin-3$^{-/-}$-mice. (A) to (C): 125 dpi and (D) to (F): terminal stage of disease.

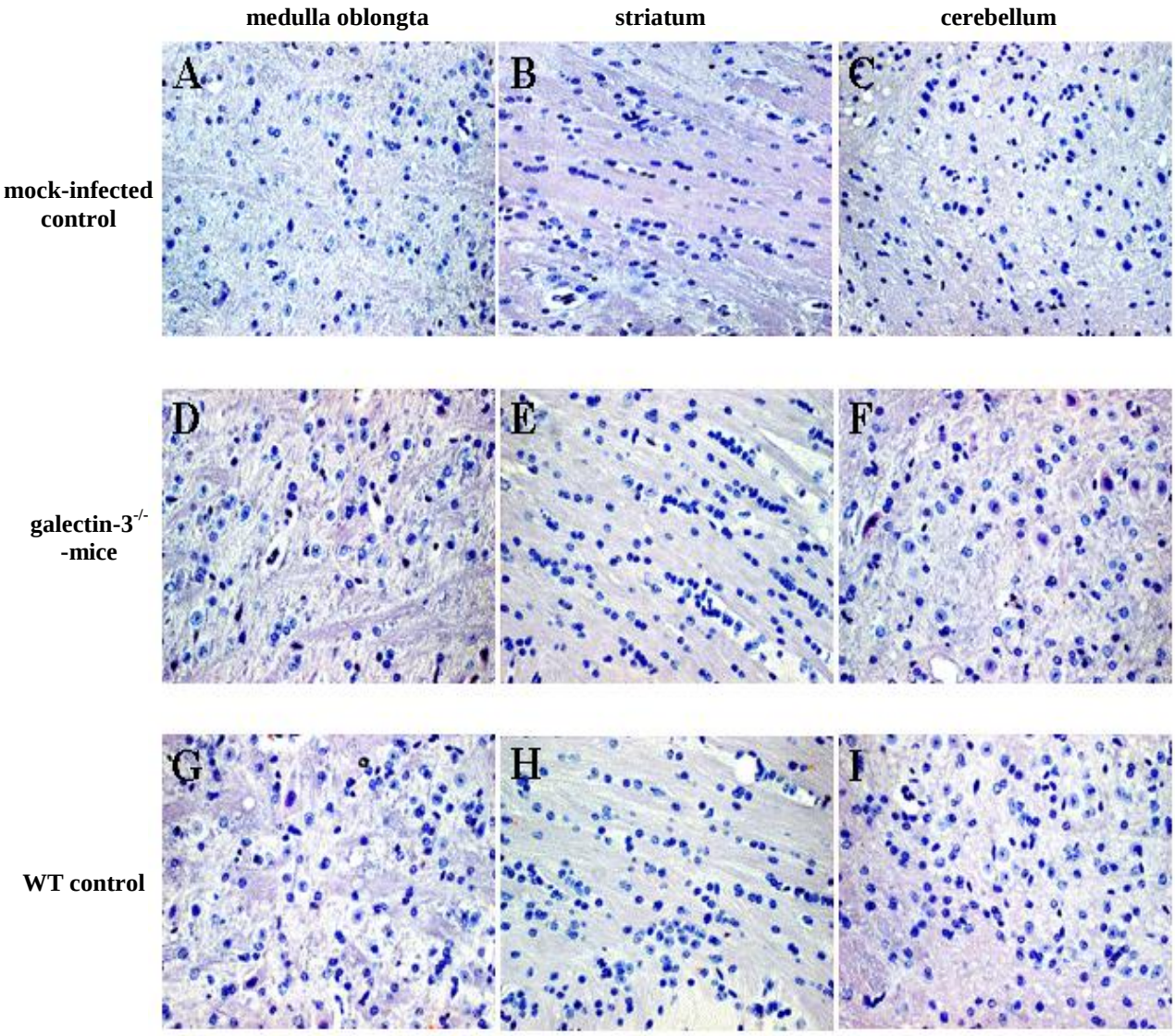

Figure 6. Immunohistochemical staining of LAMP-2-positive activated microglia at 125 dpi. (A), (D), (G): medulla oblongata, (B), (E), (H): striatum & (C), (F), (I): cerebellum, 400-fold. (A) to (C): mock-infected control, (D) to (F): Galectin-$3^{-/-}$-mice (G) to (I): WT control.

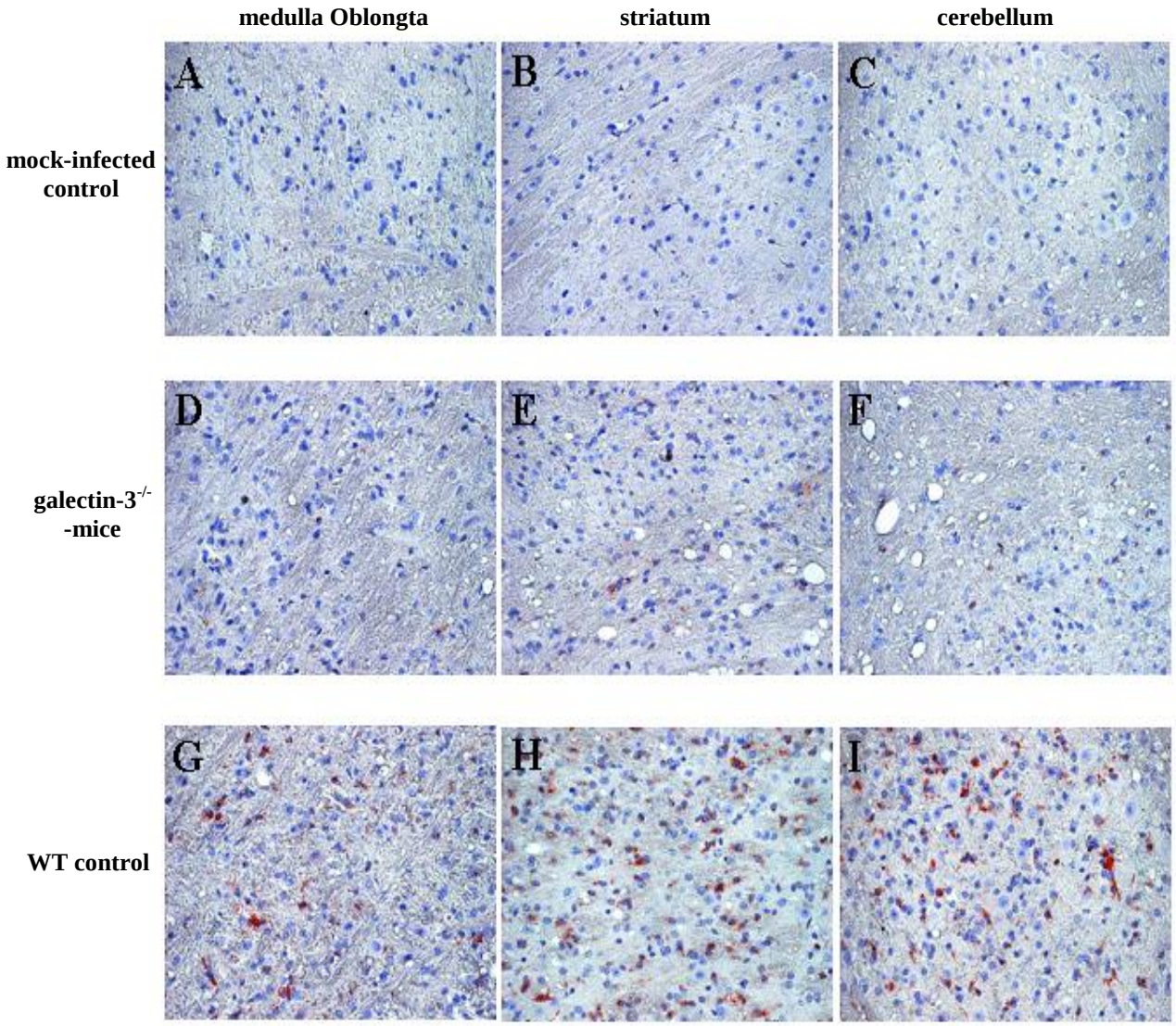

Figure 7. Immunohistochemical staining of LAMP-2-positive activated microglia at the terminal stage of disease. (A), (D), (G): medulla oblongata, (B), (E), (H): striatum & (C), (F), (I): cerebellum, 400-fold. (A) to (C): mock-infected control, (D) to (F): Galectin-3$^{-/-}$-mice (G) to (I): WT control.

4.1.7 Lamp-2 Gene Expression in Scrapie-infected CNS

Because of the differences found in LAMP-2 protein expression (section 4.1.6), possible roles of galectin-3 in Lamp-2 gene expression was further investigated by TaqMan PCR. As shown in figure 8, there were however no significant differences concerning Lamp-2 mRNA levels between galectin-$3^{-/-}$-mice and WT controls. Hence, it is possible that galectin-3 is involved in post-translational regulation of LAMP-2 protein expression in this scrapie model.

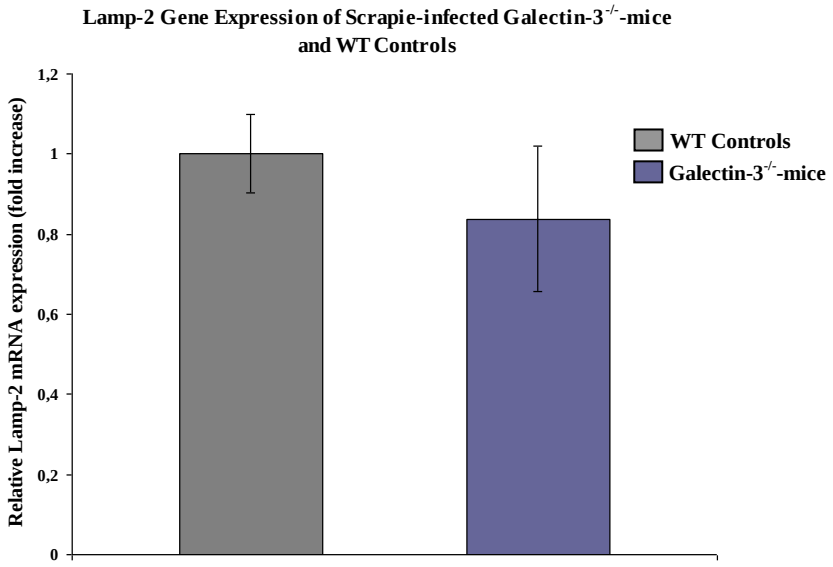

Figure 8. Lamp-2 mRNA expression of scrapie-infected galectin-$3^{-/-}$-mice and WT controls at the terminal stage of the disease relative to unifected mice.

4.1.8 Analysis of the Accumulation of Autophagic Vacuoles in Scrapie-infected CNS

LAMP-2 is critically involved in autophagy, therefore, the extent of autophagosome formation was studied [197]. LC3, a marker for autophagy, is present as LC3-I in the cytosol and, upon induction of autophagy, as phosphatidylethanolamine-conjugated LC3-II which is tightly bound to the autophagosomal membrane [198, 199]. The ratio of LC3-II to LC3-I is closely correlated with autophagosome numbers and therefore used as indicator of autophagosome formation [199]. As shown by figure 9A, two bands with 18kDa (representing LC3-I) and 16kDa (representing LC3-II) were detected by immunoblot-analysis. The relative amount of LC3-II to LC3-I (LC3-II/LC3-I) was assessed by densitometric analysis. As demonstrated in figure 9C, the extent of autophagosome formation appeared to be unaffected by the scrapie infection nor by ablation of galectin-3. The amount of protein loaded in each lane was identical as confirmed by actin blotting (figure 9B).

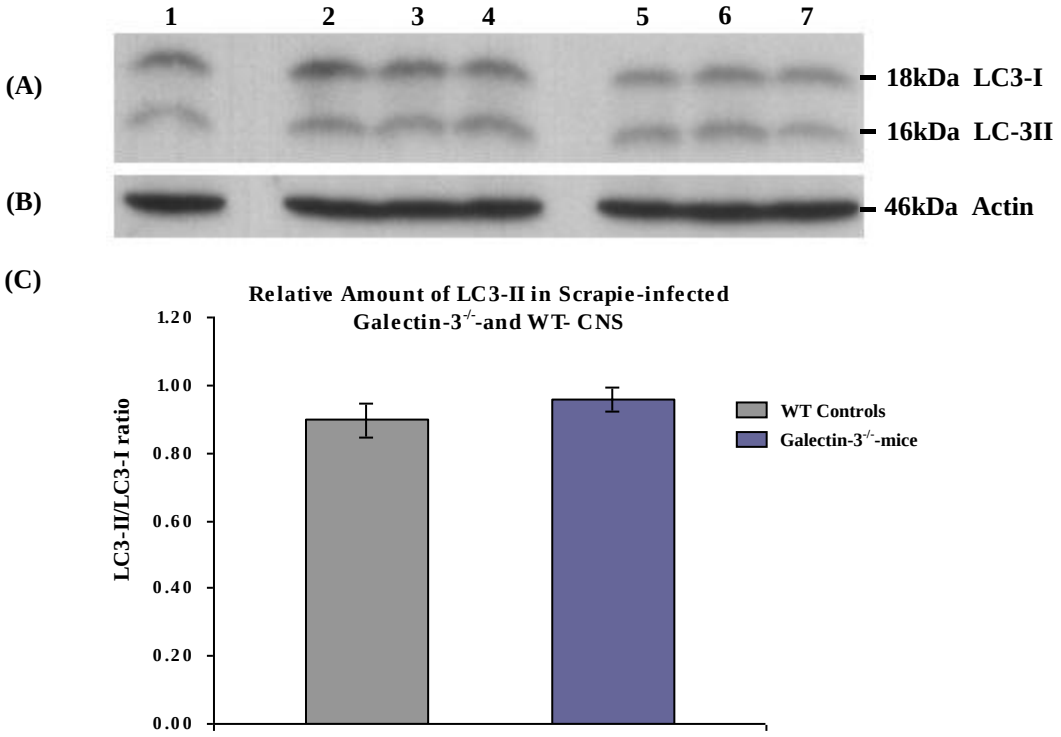

Figure 9. Western-blot detection of LC3 and LC3-II/LC3-I ratios as a measure of autophagosome formation. (A) Anti-LC3 antibody; lane 1, mock-infected control; 2-4, scrapie-infected WT controls; 5-7, scrapie-infected galectin-$3^{-/-}$-mice. (B) Anti-actin antibody as loading control. (C) LC3-II/LC3-I Ratios determined by quantitative densitometric analysis of the LC3 immunoblot.

4.1.9 Analysis of the Autophagy Related Genes in Scrapie-infected CNS

Apart from assessing the extent of autophagosome formation, expression of genes participating in autophagy induction was also examined using TaqMan PCR. As shown in figure 10, mRNA levels of Beclin-1 which promotes autophagy through the class III phosphatidylinositol 3′-kinase (PI3K) pathway [200], and of Atg5, required for formation of autophagic vacuoles [201], did not differ significantly between infected WT controls and galectin-$3^{-/-}$-mice. However, compared to the mock-infected control brains, significant downregulation of Beclin-1 (2.5 fold) and Atg5 (1.7 fold) mRNA levels was observed in scrapie infections (figure 10).

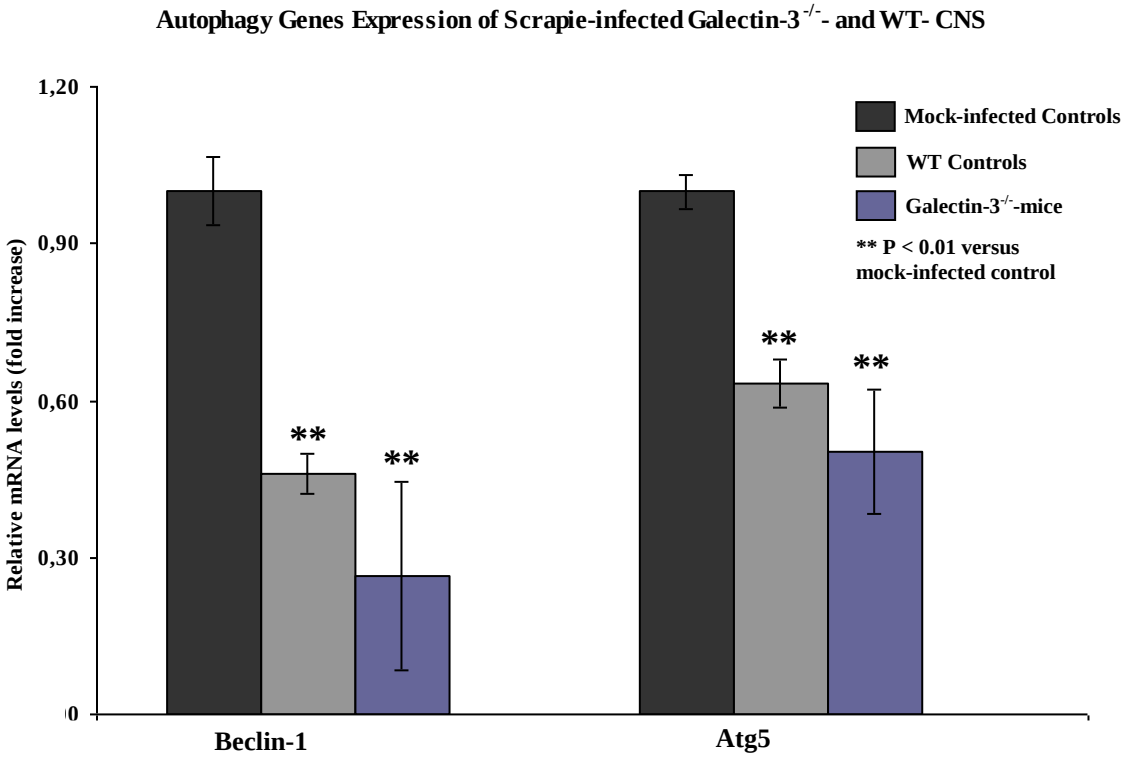

Figure 10. The mRNA expression profile of autophagy controlling genes Beclin-1 and Atg5 in scrapie infected WT controls and galectin-$3^{-/-}$-mice and mock infected control.

4.1.10 Interactions Between PrP^{Sc} and Cellular Proteins

Galectin-3 is a receptor for advanced glycation endproducts [202, 203]. Interestingly, recent findings show that PrP^{Sc} is modified by nonenzymatic glycation [204]. Based on these facts, it could be possible that galectin-3 would recognize PrP^{Sc} if modified by advanced glycation endproducts. The interactions between PrP^{Sc} and galectin-3 as well as other cellular proteins were studied by blotting the PTA precipitated brain homogenates with antibodies recognizing the proteins of interest (section 3.2.3.5). Lane 1 and 2 of figure 11 are PTA precipitates from scrapie- and mock- infected brain homogenate, respectively. Lane 3 and 4 are the corresponding total brain homogenates without prior PTA precipitation, which served as controls. Large amount of PrP^{Sc} were detected by the anti-PrP antibody 4H11 after PTA precipitation as shown in lane 1 of figure 11D. This is expected since PTA forms preferentially complexes with PrP^{Sc} but not with other proteins (section 3.2.3.5). In principle, any protein bound to or interacting with PrP^{Sc} should also be detected in the PTA precipitates. Therefore the presence of other cellular proteins in the PTA precipitated brain homogenates was examined. LAMP-1 (appearing as bands at 110kDa and 80kDa) and NeuN (appearing as bands around 70kDa and 45kDa) are strongly expressed in the CNS. They were detected in the whole brain homogenate controls for both scrapie- and mock-infected mice before PTA precipitation (lane 3 and lane 4 of figure 11A to B). However, the two proteins were undetectable in scrapie-infected PTA precipitates (lane 1 of figure 11A and B). In contrast, galectin-3 was found in the PTA-precipitated brain homogenate from a prion-infected mouse (lane 1 of figure 11C). This indicates a possible interaction of galectin-3 with advanced glycation endproducts-modified PrP^{Sc}.

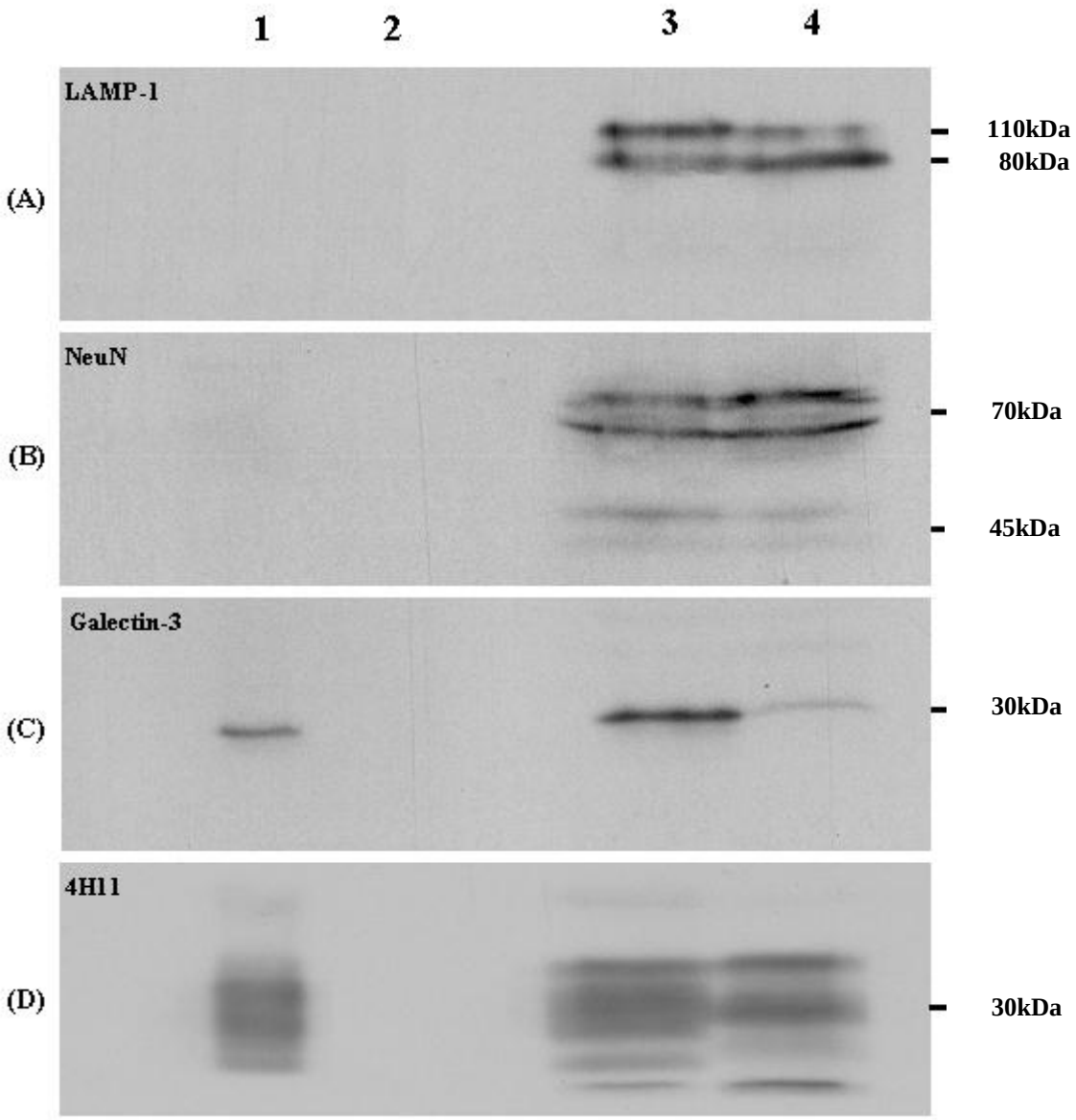

Figure 11. Western-blot of PrP^{Sc}-interacting protein. Lane 1 and 3, scrapie-infected mouse brain homogenate; lane 2 and 4, mock-infected controls. Lane 1 & 2, PTA precipitated material; lane 3 & 4; whole brain homogenate without precipitation.

4.2 Simvastatin Treatment of Scrapie-infected Mice

4.2.1 Prolonged Survival Times of Simvastatin-treated Scrapie-infected Mice

The effect of simvastatin treatment after scrapie infection was investigated using mice with C57BL/6 background as described in section 3.2.1.2. The survival time of both simvastatin-treated and untreated control mice were collected from the terminally disease stage after infection. Compared to the control groups, simvastatin-treated mice survived on average 16 ($p=0.00003$) and 20 days ($p=0.0003$) longer when challenged with 10^{-3} and 10^{-4} diluted brain homogenates, respectively (table 7). Moreover, simvastatin treatment rendered survival times of mice comparable to the controls receiving a 10 time lower infectious dose (figure 12). Simvastatin-treated mice with 10^{-3} infectious dose, died on average on 194±6 (dpi) (table 7) while corresponding untreated control, died on average on 178±7 dpi (table 7). For the groups which were infected with a 10 times lower infectious dose (i.e. 10^{-4}), simvastatin-treated mice have an average survival time of 213±9 dpi (table 7), whereas the untreated counterparts died on average 193±11 dpi (table 7). Furthermore, severe clinical symptoms like poor coat condition, hunched posture, weight loss, and behavioural changes (hyper-responsiveness to touch and nervousness) of the late stage prion infection developed identically in treated and untreated animals. However, simvastatin-treated mice reached this terminal stage of infection on average 15 days later than the controls (figure 13). Furthermore, no adverse effects of simvastatin therapy in any of the treated groups were found during the whole course of treatment.

Table 7. The survival times of simvastatin-treated mice and untreated control upon i.c. scrapie infection (dpi)

Dilution of 10% Brain homogeneate and infection route (i.c.)	Simvastatin-treated	Untreated Control
10^{-3}	**194 ± 6, (n = 10)*** (184, 185, 189, 194, 195, 196, 197, 198, 198, 203)	**178 ± 7, (n = 10)** (166, 166, 176, 177, 177, 179, 180, 184, 186, 188)
10^{-4}	**213 ± 9, (n = 10)**** (196, 205, 208, 211, 211, 212, 215, 218, 225, 228)	**193 ± 11, (n = 10)[a]** (180, 180, 183, 189, 194, 195, 201, 201, 212)

[a] One animal in this group died from causes unrelated to the scrapie infection
*** p = 0.00003 versus control group and ** p = 0.0003 versus control group**

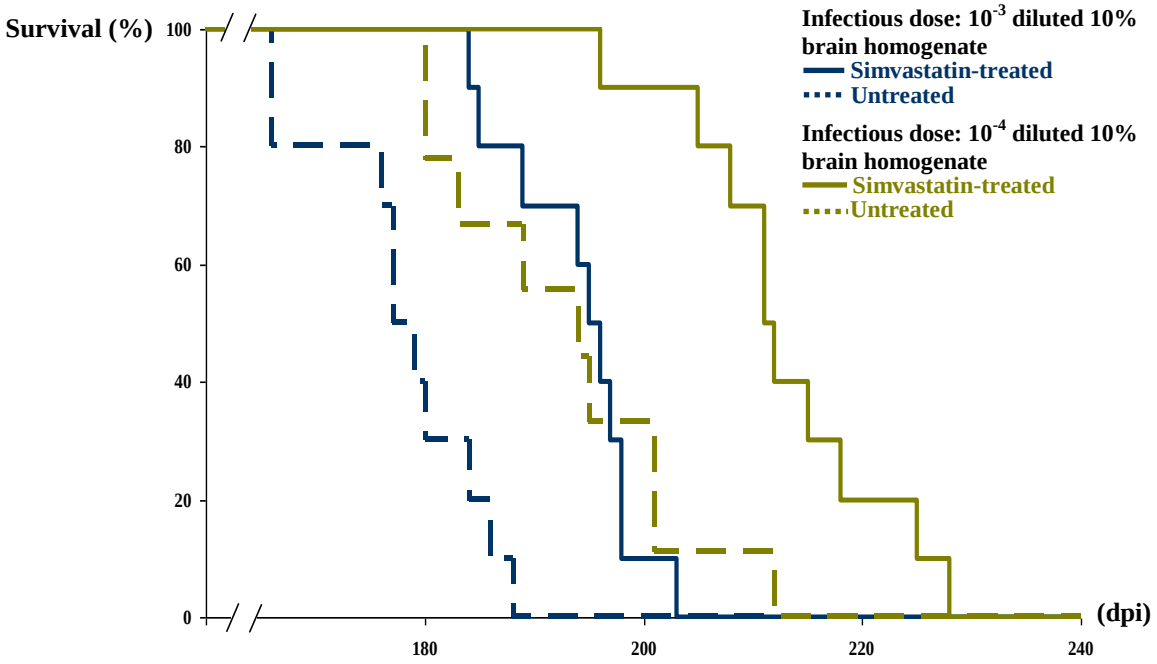

Figure 12. Survival curves of simvastatin-treated mice and untreated controls upon scrapie infection

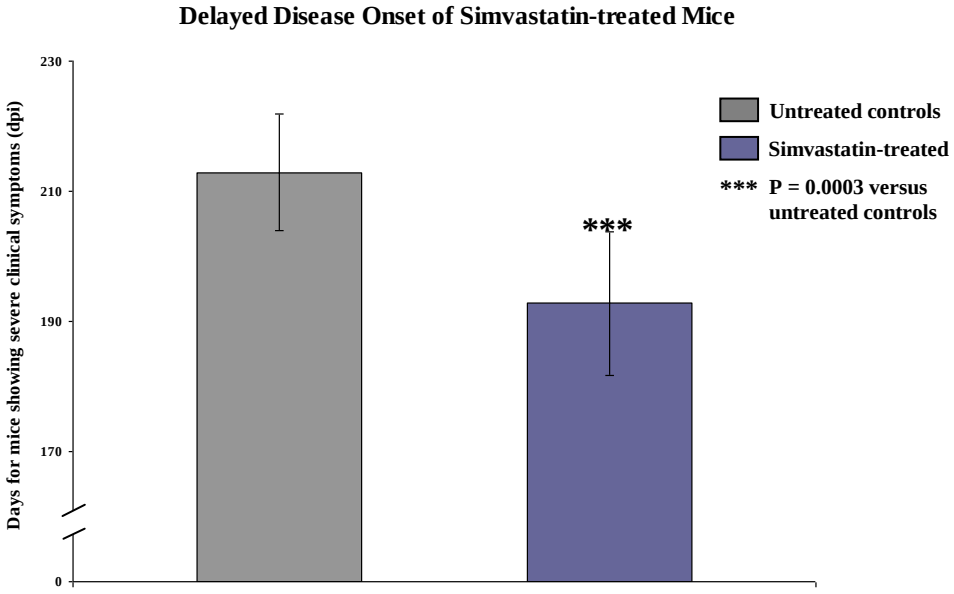

Figure 13. Averaged days before reaching terminal stage after scrapie infection in simvastatin-treated mice and untreated control

4.2.2 Effects of Simvastatin Treatment on Total Brain Level of Cholesterol, Cholesterol Precursors and Cholesterol Metabolites

Since expression of genes involved in cholesterol synthesis and transportation is dysregulated in prion-infected CNS [205, 206], the administration of cholesterol-lowering simvastatin may modulate prion pathogenesis through its action on cholesterol metabolism. The effect of simvastatin on normal brain cholesterol synthesis pathway was therefore determined by examining the total brain level of cholesterol, as well as, its metabolites and precursors of simvastatin-treated healthy C57BL/6 mice (section 3.2.1.3). No change could be found in the levels of cholesterol and its metabolites cholestanol and 24S-OH-cholesterol (24-S-OH-chol) in whole brain homogenates after 28-day treatment of the drug (table 8). However, compared to the control group, simvastatin moderately decreased the levels of the cholesterol precursor lanthosterol, lanosterol, and desmosterol by 16.6% (p=0.021), 15.3% (p=0.022) and 13.4% (p=0.033), respectively, indicating a slight downward modulation of cholesterol synthesis in the brain.

Table 8. Effects of simvastatin treatment on brain cholesterol levels

	Cholesterol (µg/mg)	**Cholestanol (ng/mg)**	**24-S-OH-chol (ng/mg)**	**Lanthosterol (ng/mg)**	**Lanosterol (ng/mg)**	**Desmosterol (ng/mg)**
Untreated (n=6)	66.4±4.6	139.6±15.9	148.7±15.3	91.2±8.8	43.6±2.9	402.7±33.8
Simvastatin (n=6)	63.7±4.6	136.5±15.9	153.2±30.3	76.1±10.2*	36.9±5.3*	348.8±41.5*

***p< 0.05 versus untreated control group (data provided by D. Lütjohann, University of Bonn)**

4.2.3 Accumulation of PrP^{Sc} After Simvastatin Treatment

To characterize prion infection of the simvastatin-treated animals in more detail, the possible simvastatin-related inhibition of PrP^{Sc} accumulation was studied using Western blotting. The deposition of PrP^{Sc} in brain tissue of the drug-treated animals and untreated controls were analysed and compared by probing the corresponding brain homogenates with antibody 4H11. As shown in figure 14, PrP^{Sc} accumulation of drug-treated animals (lane 1 of figure 14) demonstrated no difference to the untreated controls (lane 3 of figure 14). Therefore, no direct *in vivo* correlation to the reported abrogation of PrP^{Sc} deposition by cholesterol-lowering drugs in prion-infected cell cultures was demonstrated [186, 207].

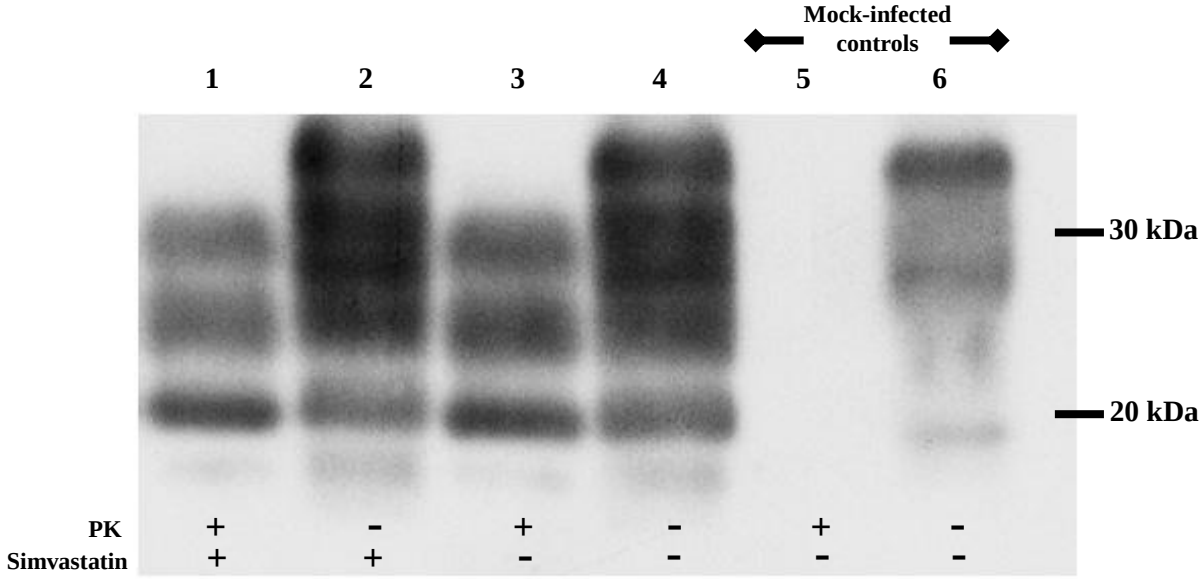

Fig 14. Western blot detection of PrP and PrP^{Sc} in brain homogenates. Lane 1-6, scrapie infected mice; lanes 5-6, mock-infected controls. Prior PK digestion was omitted in lanes 2, 4, and 6. Lanes 3 and 4:untreated controls; lanes 1, 2: simvastatin-treated mice.

4.2.4 Modulation of Glial Cells Response in Scrapie-infected CNS After Simvastatin Treatment

The expression of glial signature proteins was studied to address the disease-associated pathology and the inflammatory reactive gliosis. GFAP and Mac-3 (LAMP-2) protein expression were analysed as typical astrocyte- and microglia- specific activation markers, respectively. For both proteins, the staining intensities in prion-infected mice were similar with or without simvastatin treatment. Therefore, simvastatin did not promote general downregulation of glia activation in prion-infected CNS (figure 15A to F). However, in agreement with the described inhibition of MHC-II expression by HMG-CoA reductase inhibitors, a 4- to 5- fold reduction of MHC class II-positive cell numbers was observed (figure 15G to I). The immunoreactivity for galectin-3 was also tested. Galectin-3 expression is upregulated in scrapie-infected brain on both the mRNA [193] and protein level (section 4.1.1). As shown in figure 15J to L, the immunohistochemical galectin-3 detection confirmed the gene array data. In mock-infected healthy brain tissue galectin-3 expression was almost absent, whereas in scrapie-infected brains the protein became readily detectable. Interestingly, the galectin-3 overexpression was 2- to 3-fold more strongly elevated upon simvastatin-treatment (figure 15J to L).

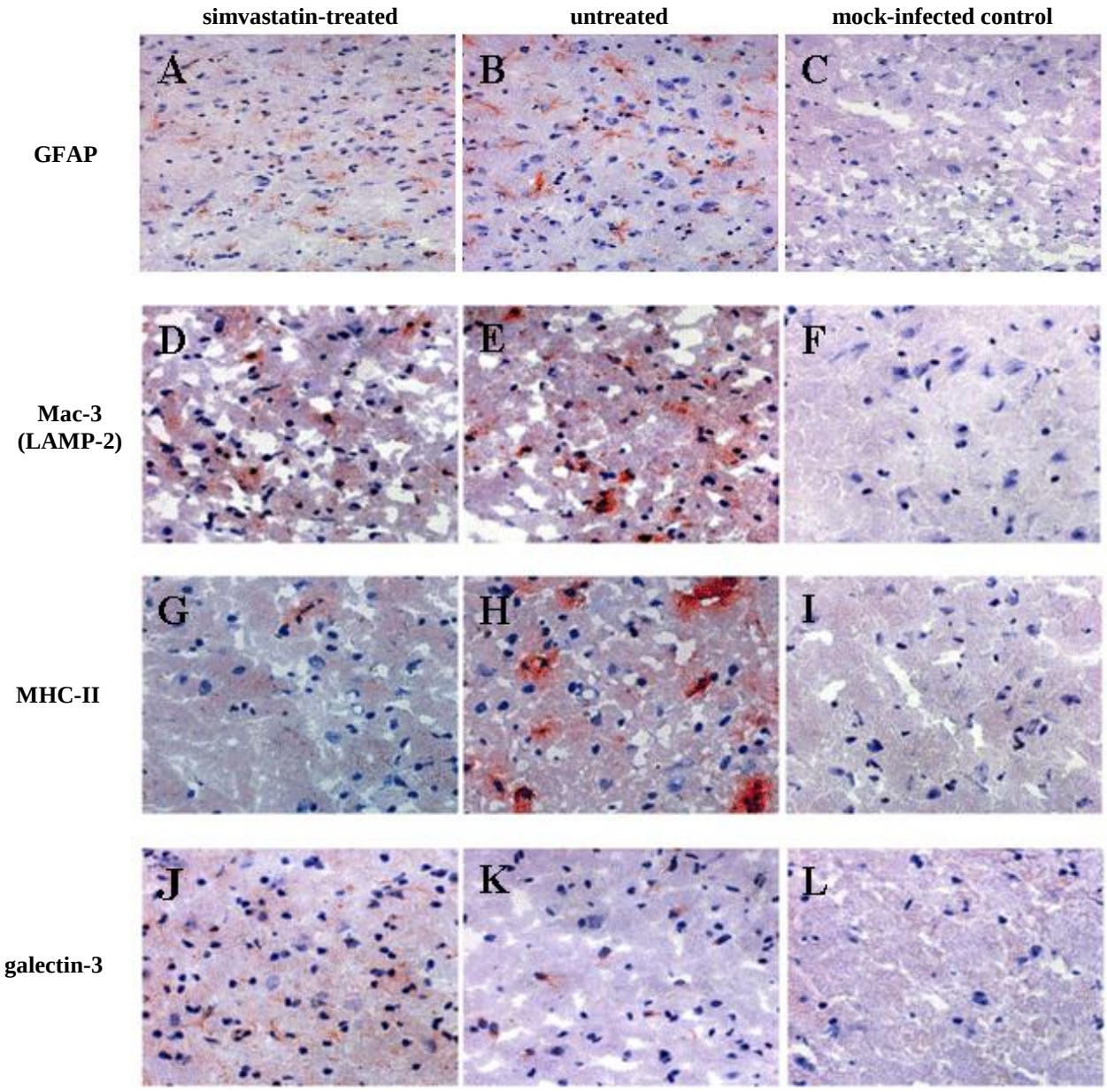

Figure 15. Immunohistochemical protein expression analysis of disease-associated gliosis. (Left) simvastatin-treated, (middle) untreated, and (right) mock-infected mice. Analysed marker proteins were GFAP (A) to (C), Mac-3 (LAMP-2) (D) to (F), MHC-II (G) to (I), and galectin-3 (J) to (L).

5 Discussion

Prion diseases are fatal and at present there are neither cures nor palliative therapies available. Therefore, the understanding of the pathomechanism and search for effective interventions for prion diseases are of great importance. Since different neurodegenerative diseases share similarities in pathology at the molecular level, findings in prion diseases may in principal shed light on other neurodegenerative protein misfolding diseases.

Galectin-3, a proinflammatory mediator, participates extensively in the homeostasis of immune system (section 1.4.3). Recently, it has been suggested as a novel target for anti-inflammatory drugs [151]. Furthermore, the overexpression of galectin-3 in scrapie-infected brain tissue has been detected [193]. Based on these findings, the possible role of galectin-3 in chronic neurodegeneration was examined by characterizing the scrapie-infected galectin-$3^{-/-}$-mice in the present study. The possible effects of immunomodulatory/anti-inflammatory drugs on the profile of scrapie-induced galectin-3 expression, as well as, on prion pathogenesis were also examined. Among different available drugs and compounds, statins are of particular interest because of their *in vitro* anti-prion effects and potential immunomodulatory properties (section 1.5.2). In this study, the effects of simvastatin on scrapie-infected WT mice were evaluated. The lipophilic drug was chosen because it can reach beyond the BBB.

5.1 Galectin-3 Ablation Experiment

5.1.1 The Survival Times of Scrapie-infected Galectin-$3^{-/-}$-Mice

Ablation of galectin-3 promoted a significant increase in survival time by up to three weeks upon exposure to the scrapie agent (table 5). The roughly equal effect of galectin-3-deficiency on survival time upon i.c. and i.p. challenges indicated that galectin-3 is probably not involved in peripheral prion spread and subsequent neuroinvasion. Initial prion binding or uptake facilitating further spread towards lymphnodes was attributed to resident macrophage, dendritic cells, and neutrophils [208-211]. The data shown here indicated that the reported impairment of peritoneal macrophage response by ablation of galectin-3 had no major influence on the outcome of the i.p. infections.

5.1.2 Activation of Astrocytes and PrP^{Sc} Accumulation

To further probe for the functions of galectin-3 in the CNS, typical parameters of prion infections, such as PrP^{Sc} deposition and astrocytosis, were characterized by comparing the knockout mice to WT controls. As indicated by the immunohistochemical analysis of GFAP protein expression (figure 4), the extent of the astrocytosis appeared not to be affected by galectin-3 ablation in both the early and terminal disease stages. The extent of PrP^{Sc} deposition of scrapie-infected galectin-$3^{-/-}$- mice appeared not to be affected either. No changes of PrP^{Sc} accumulation could be found in both early time point and the terminal disease stage as indicated by PET-blotting (figure 3). Therefore, the beneficial effects (i.e. prolonged survival times) are unlikely to be due to changes of astrocytic activities or changes in PrP^{Sc} deposition.

5.1.3 Microgliosis

Given that in our model galectin-3 was predominantly expressed by activated microglia (figure 2), this cell type was examined more. The activated microglia marker, LAMP-2, was studied. At the early disease stage, LAMP-2 expression was absent (figure 6). However, at the terminal disease stage, a strong induction of LAMP-2 in scrapie-infected WT mice was observed. Surprisingly, in the absence of galectin-3, nearly no LAMP-2 expression was detected (figure 7). The detected upregulation of LAMP-2 in the WT controls is in good agreement with the previously observed dysregulation of endosomal/lysosomal system (ELS) during prion infections of the CNS. Abnormally large amount of PrP^{Sc}-containing endosomal/lysosome-related structures has been reported in neuronal cell processes after prion infection [212]. In addition, genes encoding lysosomal hydrolases and lysosome-associated multitransmembrane protein (LAPTm5) are upregulated in prion-infected brain tissue [205, 213]. Interestingly, galectin-3 was previously shown to interact directly with LAMP-2 [159] and this may suggest that the observed lack of LAMP-2 induction in galectin-$3^{-/-}$-mice could be due to the loss of this interaction resulting in increased LAMP-2 protein turnover. Quantitative RT-PCR-based expression analysis demonstrated similar Lamp-2 mRNA levels in galectin-$3^{-/-}$-mice and WT controls (figure 8) further supporting the idea of galectin-3 control on LAMP-2 protein levels but not Lamp-2 gene expression.

5.1.4 Galectin-3 and Autophagy in Prion Diseases

As mentioned in section 5.1.3, the downregulated LAMP-2 expression in scrapie-infected galectin-$3^{-/-}$-mice points towards the involvement of ELS in prion diseases. In fact, the endosomal/lysosomal pathway is generally thought to be involved in turnover and generation of misfolded protein aggregates and was also implicated in the pathogenesis of other neurodegenerative disorders like Alzheimer's disease [214]. Additionally, LAMP-2 is also critically involved in autophagy, a lysosomal pathway for degrading organelles and long-lived proteins, which participates actively in physiological but also pathological conditions including chronic neurodegeneration [197, 215]. Therefore, components involved in autophagy in our scrapie model were further analysed. Interestingly, LC3-II/LC3-I ratios remained unchanged in uninfected and scrapie-infected WT- or galectin-$3^{-/-}$-mice indicating no general increase or decrease of autophagosome numbers (figure 9C). However, downregulation of genes regulating autophagy, Beclin-1 and Atg5, in scrapie-infected brain tissue was evident (figure 10). As yet, the role of autophagy in chronic neurodegeneration appears to be complex. Autophagy represents a pathway towards programmed cell death and could thereby theoretically contribute to neuronal loss in chronic neurodegeneration. In fact, autophagy has been implicated as mechanism of neurodegeneration in prion diseases [216]. On the other hand, impairment of autophagy is clearly associated with neuronal death and neurological abnormalities [217, 218]. Hence, autophagy is essential for maintenance of normal CNS functions. The lower expression levels of Beclin-1 and Atg5 observed here would therefore suggest that downregulation or disturbance of autophagy is part of the pathogenic process in prion infections of the CNS. Therefore, the findings are in support of the idea that reduced or defective autophagy, rather than excessive autophagy, in combination with endosomal/lysosomal dysfunction may contribute to chronic neurodegeneration.

5.1.5 Interaction Between Galectin-3 and Prion Protein

PTA precipitation was used to purify and enrich PrP^{Sc} from scrapie-infected whole brain homogenate. This procedure yielded a significant amount of PrP^{Sc} from the brain homogenate in the precipitation product as shown in western blots probed with 4H11 (Figure 11D lane 1 & 3). The idea that protein complex with PrP^{Sc} would also be precipitated out was the basis for the study of prion protein interactions. To confirm specificity of the precipitation, NeuN and

LAMP-1 which are expressed in brain tissue, were not detected in scrapie-infected PTA precipitates suggesting that they did not interact with PrP^{Sc} and were thus removed by the PrP^{Sc}-specific PTA purification. In contrast, galectin-3 was detected in both scrapie-infected whole brain homogenate and PTA precipitates. This result suggests a direct- or indirect- interaction between galectin-3 and PrP^{Sc}. The weaker galectin-3 signal in the PTA precipitate compared to the whole brain homogenate (figure 11C) suggests however that only a fraction of the total amount of galectin-3 was retained in the precipitate.

Galectin-3 is a receptor for advanced glycation endproducts (AGEs) [202, 203]. AGEs are the irreversible products of Maillard reaction (diagram 5) involving non-enzymatic glycation and oxidation processes between carbohydrates and amino groups of proteins and lipoproteins. Apart form galectin-3, other suggested AGE-binding proteins include the receptor of advanced glycation endproduct (RAGE) [219], class B scavenger receptors CD36, class A macrophage scavenger receptor type I and II [220-223], AGE-R1 and AGE-R2 [224]. The Maillard reaction begins with the formation of a reversible product - Schiff base, which undergoes a series of intermolecular rearrangements, dehydrations and condensations to become the Amadori product and finally AGEs [225]. The AGEs consist of a heterogeneous class of compounds including carboxymethyllysine (CML), carboxyethyllysine (CEL), pentosidine, furosine and the methylglyoxal-derived Argpyrimidine [226, 227].

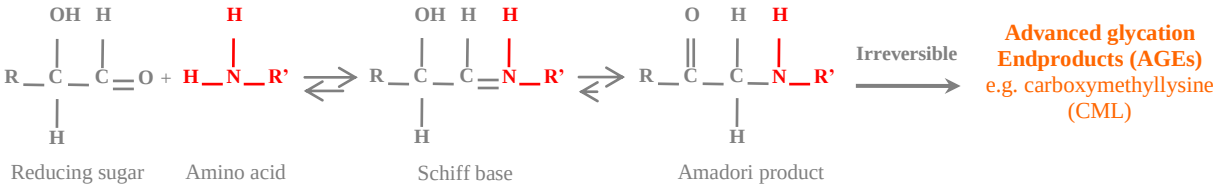

Diagram 4. Simplified pathway of Maillard reaction

The amount of AGEs formed on a protein depends on the half-life of that particular protein. In fact, AGEs are frequently found on long-lived proteins, for example collagen and lens crystalline, which are associated with ageing [228-230]. The accumulation of AGE also depends on glucose concentration of the microenvironment. In the case of diabetes mellitus induced hyperglycemia, nonenzymatic glycation is enhanced and is related to the pathogenesis of diabetic complications like neuropathy [231, 232]. AGEs are also participants of other pathological conditions involving chronic inflammation such as rheumatoid arthritis [233]. The

interactions between AGEs and some of its receptors, for example RAGE, induce cell activations, which lead to dysregulated tissue remodelling. On the others hand, some of these AGE-receptors-mediated pathways protect tissues from AGEs damages by mediating the removal process of glycated molecules [227]. Intriguingly, galectin-3 also plays critical roles in diseases involving AGEs formation. In a study using galectin-$3^{-/-}$-mice, an accelerated diabetic glomerulopathy and increased AGEs accumulation were found in the knockout animals when compared to the WT counterparts [234]. These findings suggested that the interactions between galectin-3 and AGEs play a role in disorders involving glycated molecules. Since the N-terminus of PrP^{Sc} is AGEs-modified, galectin-3 could potentially recognize PrP^{Sc} as such [204]. In addition, galectin-3 may associate with PrP^{Sc} indirectly through the binding to other proteins for example in lipid rafts [33]. Other possible participants include very low density lipoprotein (VLDL) and low density lipoprotein (LDL), which are known binding partners of PrP^{Sc} [235]. However, possible interactions between galectin-3 and these proteins remain to be elucidated.

Although galectin-3 was shown recently to participate in endocytosis of AGEs [236], this is not the case in our disease model as demonstrated by the similar accumulation of PrP^{Sc} in galectin-$3^{-/-}$-mice and WT controls. The prolonged survival times upon scrapie-infection after galectin-3 ablation revealed a deleterious role of the protein in prion pathogenesis. The downregulated microgliosis of the scrapie-infected galectin-$3^{-/-}$-mice further suggest an immunomodulatory effect of these interactions between galectin-3 and PrP^{Sc} during the course of prion diseases development. The involvement of AGEs in other neurodegenerative protein misfolding disorders, for example, Alzheimer disease, has also been reported and is related to the AGEs-induced oxidant stress and dysregulated microglia activation [237-239].

5.2 Simvastatin Treatment of Scrapie-infected mice

5.2.1 The Survival Times of Scrapie-infected WT Mice After Simvastatin Treatment

Simvastatin treatment delayed disease progression and prolonged survival time of scrapie-infected mice up to 18 days in established prion infections of the CNS. Treatment commenced 100 dpi, a stage in which accumulation of PrP^{Sc}, inflammation, glia activation, and neurodegeneration are already evident [106, 205, 240]. Moreover, clear indications of behavioural changes have been reported for this stage of infections indicating therapeutic efficacy of simvastatin well towards the symptomatic stage of the disease [241-243]. Moreover,

simvastatin treatment rendered survival times of mice comparable to the controls receiving a 10 times lower infectious dose (194 versus 193 days, p= 0.39, figure 12), which further underlines the significance of the therapeutic effect.

5.2.2 Effect of Simvastatin on Scrapie-induced Glia Activation and PrP^{Sc} Accumulation

In view of the significantly prolonged survival time of the simvastatin-treated animals, glia activation and PrP^{Sc} deposition in simvastatin-treated mice were compared to the controls. After treatment, no measurable reduction of PrP^{Sc} levels in brain tissue of prion-infected mice could be found (figure 14). Therefore, simvastatin appeared not to be affecting the level of PrP^{Sc} accumulation *in vivo*, although *in vitro* studies showed that HMG-CoAR inhibitors as well as squalene synthase suppress PrP^{Sc} deposition in prion-infected cell cultures [186, 207]. Similarly, analysis of inflammatory glia activation shows no overt effect of simvastatin on the expression of typical activation markers. Neither GFAP nor LAMP-2 protein expression was significantly affected by statin therapy (figure 15A & B; D & E). However, glia MHC-II expression was 4 to 5 times lower in the statin-treated group (figure 15G & H). The reduced MHC-II expression found in the simvastatin-treated group is in agreement with findings demonstrating the inhibitory effects of simvastatin on MHC-II expression by modulating the expression level of CIITA, a transcription factor required MHC-II gene expression [244, 245]. Moreover, galectin-3 expression level was found to be significantly elevated after simvastatin treatment (figure 15J & K). These findings indicate that despite general activation, glial functions are indeed affected and conversely down or upregulated by simvastatin (figure 15).

5.2.3 The Immunomodulatory Effects of Simvastatin on Prion Diseases

Although *in vitro* studies demonstrated that the anti-prion activities of statin are linked to lowering cellular cholesterol levels, the situation *in vivo* is obviously more complex [186, 207]. A recent array-based expression analysis showed that genes encoding proteins involved in cholesterol synthesis, including HMG-CoAR and squalene synthase, are downregulated and genes participating in cholesterol efflux (e.g., adenosine triphosphate binding cassette, subfamily A, member 1) are induced in human and murine prion-infected brain tissue [205-207]. Statin-treatment could therefore theoretically aggravate this specific condition by an additional inhibition of normal neuronal cholesterol synthesis. However, the study here shows that even

the applied high-dose simvastatin regimen did not affect brain levels of cholesterol and its metabolites cholestanol and 24S-OH-chol (Table 7), despite a mild reduction of cholesterol precursor lanthosterol, lanosterol, and desmosterol levels. Hence, the results do not substantiate concerns about statin use and possibly associated detrimental effects on brain cholesterol levels. Moreover, taking into account the very long brain cholesterol half-life times (e.g., at least 5 years in humans), it appears unlikely that the therapeutic benefit of simvastatin observed in this study is due to its cholesterol-lowering activity [246]. Likewise, as shown in section 4.2.3, simvastatin-treatment did not induce a measurable reduction of PrP^{Sc} levels in brain tissue of prion-infected mice, whereas inhibition of cholesterol synthesis prevents prion replication *in vitro* [186, 207].

A wide spectrum of anti-inflammatory effects of statins in addition to their cholesterol-lowering action has been described (section 1.5.2). This immunomodulatory effects could be related to the inhibited production of non-sterol isoprenoids such as, farnesyl pyrophosphate (FPP) and geranylgeranyl pyrophosphate (GGPP) in the cholesterol biosynthetic pathway [247]. Isoprenylation is a process in which FPP or GGPP are added to a protein and the isoprenylated products play vital roles in membrane attachment and inflammation [248, 249]. Members of the Ras superfamily of GTPases, for example, Rho are isoprenylated [250]. Therefore, the immunomodulatory effects of statins could probably be mediated by modifying the isoprenylation of these small GTPases. Recently, it has been reported that the effects of statins in experimental autoimmune encephalomyelitis (EAE) animal models are mostly attributed to a statin-induced shift of proinflammatory to anti-inflammatory conditions [190, 251]. However, the statins-induced immunomodulatory effects could also be a result of direct inhibition of the leukocyte function antigen-1 (LFA-1)/ICAM-1 interaction, which is independent of cholesterol synthesis [188].

5.2.4 Simvastatin for Treatment of Prion Diseases

Although different methods or compounds interfering prion replication have been introduced as therapeutic strategies (section 1.5.1), current therapeutic possibilities for treatment of prion diseases are extremely limited. Proven inhibitors of prion replication like PPS do not reach beyond the BBB and have to be administered through chirurgical implantation of catheters to facilitate drug supply into the brain by pumps [184, 252]. Besides PPS, only the drugs dapsone,

amphotericin B, and the amphotericin B-derivative MS-8209 have been described to delay disease progression upon intracerebral inoculation of the scrapie agent [184, 253, 254]. However, dapsone treatment was started immediately after the infection, which is an unrealistic scenario, and the therapeutic benefit could not be confirmed in another prion disease model [255]. For amphotericin B, even direct infusion into brains of prion-infected animals at late stages of the disease was ineffective and no therapeutic benefit was observed when treating Creutzfeldt-Jakob disease (CJD) patients [184, 256] Moreover, application of the drug is problematic due to its toxicity [257]. In contrast, clinical use of statins over almost two decades has confirmed their well-acceptable safety profile [258]. Hence, the experimental model in this study suggests that neuroinflammation represents a rational target for therapeutic approaches of prion diseases and the use of simvastatin in cases of known genetic predispositions for development of CJD.

5.3 Outlook

This study demonstrated a therapeutic benefit of simvastatin in treatment of prion infection of the CNS. However, means to improve the efficacy of the drug should be further investigated. Compounds with inhibitory effects on amyloid formation/protein aggregation or anti-inflammatory properties could, in principal, enhance the effects of simvastatin. For example, doxycycline, a member of the tetracycline antibiotics group, is a potential candidate to be examined in combination with simvastatin. *In vitro* studies showed that doxycyline interacts with PrP^{Sc} and renders the protease-resistance of the protein in a does-dependent manner. In addition, doxycyline also diminishes prion infectivity as demonstrated by delayed onset of clinical symptoms and prolonged survival time of the animals inoculated by doxycyline-treated PrP^{Sc} inoculums [259]. On the other hand, a group of terpenophenolic compounds called cannabinoids presents in cannabis plant is another ideal candidate to be tested together with simvastatin. Thus far, two known subtypes of receptors for cannabinoids, namely CB1 and CB2, have been reported. CB1 is highly expreesed in the CNS [260, 261] while CB2 is mostly restricted to the cells of the immune system [262]. Intriguingly, CB2 is also expressed by a subpopulation of microglia in the CNS [263]. Therefore, both CB1 and CB2 could play vital roles in the process of neuroinflammation and neuroprotection. In fact, both *in vitro* and *in vivo* data suggested cannabinoids-induced CB2 activation can inhibit activation, cytokine release and

migration of microglia [264, 265]. Recent findings also demonstrated the protective role of cannabinoids, which is mediated by CB1, in some neurodegenerative conditions [266, 267].

Furthermore, the mechanisms of the immunomodulatory actions of simvastatin should also be dissected. In particular, the drug effects caused by inhibition of the LFA-1/ICAM-1 interaction should be clarified (section 5.2.4) using LFA-1 deficient mice and/or drugs selectively inhibiting LFA-1 actions. On the other hand, findings in this study showed modulatory effects of simvastatin on galectin-3 expression, which may further regulate the ELS during prion pathogenesis as demonstrated by the hampered LAMP-2 expression in the galectin-3 ablation experiment (section 5.1.3). Since expressions of lysosozymes such as cathepsin B and L, which are able to degrade PrP^{Sc} *in vitro* [268, 269], depend on the proper functioning of ELS, the potential effects of simvastatin on these endosomal/lysosomal proteases are of interest. In addition, prion-induced autophagic changes are reported in this study and appear to be protective. However, the exact roles of this cellular process in the pathomechanism are still largely unknown. Investigations using autophagy inducer such as lithium could provide a novel insight for the search of interventions for prion diseases [270].

Evidence from present study supporting modulations of prion-stimulated inflammatory responses as an effective therapeutic strategy suggests the search for other proinflammatory mediators as potential therapeutic targets. Similarly, the beneficial effects of simvastatin encourage the studies of other immunomodulatory drugs to treat prion diseases.

6 References

1. Prusiner, S.B., *Novel proteinaceous infectious particles cause scrapie.* Science, 1982. **216**(4542): p. 136-44.

2. Parry, H., *scrapie disease in sheep - historical, clinical, epidemiological, pathological and practical aspects of the natural disease.* Academic Press London, 1983.

3. Spraker, T.R., et al., *Spongiform encephalopathy in free-ranging mule deer (Odocoileus hemionus), white-tailed deer (Odocoileus virginianus) and Rocky Mountain elk (Cervus elaphus nelsoni) in northcentral Colorado.* J Wildl Dis, 1997. **33**(1): p. 1-6.

4. Williams, E.S. and M.W. Miller, *Chronic wasting disease in deer and elk in North America.* Rev Sci Tech, 2002. **21**(2): p. 305-16.

5. Creutzfeldt, H., *Über eine eigenartige herdförmige erkrankung des zentralnervensystems.* Z Ges Neurol Psychiatry, 1920. **57**: p. 1 - 18.

6. Jakob, A., *Über eigenartige erkrankungen des zentralnervensystems mit bemerkenswerten anatomischen befunden (spastische pseudosklerose-encephalomyopathie mit disseminierten degenerationsherden).* Z Ges Neurol Psychiatry, 1921. **64**: p. 147 - 228.

7. Johnson, R.T., *Prion diseases.* Lancet Neurol, 2005. **4**(10): p. 635-42.

8. Gajdusek, D.C. and V. Zigas, *Degenerative disease of the central nervous system in New Guinea; the endemic occurrence of kuru in the native population.* N Engl J Med, 1957. **257**(20): p. 974-8.

9. Gajdusek, D.C., *Unconventional viruses and the origin and disappearance of kuru.* Science, 1977. **197**(4307): p. 943-60.

10. Gajdusek, D.C., C.J. Gibbs, and M. Alpers, *Experimental transmission of a Kuru-like syndrome to chimpanzees.* Nature, 1966. **209**(5025): p. 794-6.

11. Bruce, M.E., et al., *Transmissions to mice indicate that 'new variant' CJD is caused by the BSE agent.* Nature, 1997. **389**(6650): p. 498-501.

12. Hill, A.F., et al., *The same prion strain causes vCJD and BSE.* Nature, 1997. **389**(6650): p. 448-50, 526.

13. Aguzzi, A. and C. Weissmann, *Spongiform encephalopathies: a suspicious signature.* Nature, 1996. **383**(6602): p. 666-7.

14. Manetto, V., et al., *Fatal familial insomnia: clinical and pathologic study of five new cases.* Neurology, 1992. **42**(2): p. 312-9.

15. Oesch, B., et al., *A cellular gene encodes scrapie PrP 27-30 protein.* Cell, 1985. **40**(4): p. 735-46.

16. Gerstmann, J., Sträussler, E, Scheinker, I, *Über eine eigenartige hereditär-familiäre Erkrankung des zentralnervensystems. Zugleich ein Beitrag zur frage des vorzeitigen lokalen Altern.* Z neurol, 1936. **154**: p. 736 - 62.

17. Collinge, J., M.S. Palmer, and A.J. Dryden, *Genetic predisposition to iatrogenic Creutzfeldt-Jakob disease.* Lancet, 1991. **337**(8755): p. 1441-2.

18. Dlouhy, S.R., et al., *Linkage of the Indiana kindred of Gerstmann-Straussler-Scheinker disease to the prion protein gene.* Nat Genet, 1992. **1**(1): p. 64-7.

19. Owen, F., et al., *Codon 129 changes in the prion protein gene in Caucasians.* Am J Hum Genet, 1990. **46**(6): p. 1215-6.

20. Palmer, M.S., et al., *Homozygous prion protein genotype predisposes to sporadic Creutzfeldt-Jakob disease.* Nature, 1991. **352**(6333): p. 340-2.

21. Shibuya, S., et al., *Protective prion protein polymorphisms against sporadic Creutzfeldt-Jakob disease.* Lancet, 1998. **351**(9100): p. 419.

22. Zeidler, M., et al., *Codon 129 genotype and new variant CJD.* Lancet, 1997. **350**(9078): p. 668.

23. Wopfner, F., et al., *Analysis of 27 mammalian and 9 avian PrPs reveals high conservation of flexible regions of the prion protein.* J Mol Biol, 1999. **289**(5): p. 1163-78.

24. Antoine, N., et al., *Differential expression of cellular prion protein on human blood and tonsil lymphocytes.* Haematologica, 2000. **85**(5): p. 475-80.

25. Cashman, N.R., et al., *Cellular isoform of the scrapie agent protein participates in lymphocyte activation.* Cell, 1990. **61**(1): p. 185-92.

26. DeArmond, S.J., et al., *Changes in the localization of brain prion proteins during scrapie infection.* Neurology, 1987. **37**(8): p. 1271-80.

27. Harris, D.A., *Cellular biology of prion diseases.* Clin Microbiol Rev, 1999. **12**(3): p. 429-44.

28. Kretzschmar, H.A., et al., *Scrapie prion proteins are synthesized in neurons.* Am J Pathol, 1986. **122**(1): p. 1-5.

29. Stahl, N., et al., *Scrapie prion protein contains a phosphatidylinositol glycolipid.* Cell, 1987. **51**(2): p. 229-40.

30. Turk, E., et al., *Purification and properties of the cellular and scrapie hamster prion proteins.* Eur J Biochem, 1988. **176**(1): p. 21-30.

31. Haraguchi, T., et al., *Asparagine-linked glycosylation of the scrapie and cellular prion proteins.* Arch Biochem Biophys, 1989. **274**(1): p. 1-13.

32. Tsui-Pierchala, B.A., et al., *Lipid rafts in neuronal signaling and function.* Trends Neurosci, 2002. **25**(8): p. 412-7.

33. Taylor, D.R. and N.M. Hooper, *The prion protein and lipid rafts.* Mol Membr Biol, 2006. **23**(1): p. 89-99.

34. Mouillet-Richard, S., et al., *Signal transduction through prion protein.* Science, 2000. **289**(5486): p. 1925-8.

35. Schneider, B., et al., *NADPH oxidase and extracellular regulated kinases 1/2 are targets of prion protein signaling in neuronal and nonneuronal cells.* Proc Natl Acad Sci U S A, 2003. **100**(23): p. 13326-31.

36. Carimalo, J., et al., *Activation of the JNK-c-Jun pathway during the early phase of neuronal apoptosis induced by PrP106-126 and prion infection.* Eur J Neurosci, 2005. **21**(9): p. 2311-9.

37. Thellung, S., et al., *p38 MAP kinase mediates the cell death induced by PrP106-126 in the SH-SY5Y neuroblastoma cells.* Neurobiol Dis, 2002. **9**(1): p. 69-81.

38. Carleton, A., et al., *Dose-dependent, prion protein (PrP)-mediated facilitation of excitatory synaptic transmission in the mouse hippocampus.* Pflugers Arch, 2001. **442**(2): p. 223-9.

39. Kanaani, J., et al., *Recombinant prion protein induces rapid polarization and development of synapses in embryonic rat hippocampal neurons in vitro.* J Neurochem, 2005. **95**(5): p. 1373-86.

40. Jeffrey, M., et al., *Sites of prion protein accumulation in scrapie-infected mouse spleen revealed by immuno-electron microscopy.* J Pathol, 2000. **191**(3): p. 323-32.

41. Russelakis-Carneiro, M., et al., *Prion replication alters the distribution of synaptophysin and caveolin 1 in neuronal lipid rafts.* Am J Pathol, 2004. **165**(5): p. 1839-48.

42. Brown, D.R., et al., *Prion protein-deficient cells show altered response to oxidative stress due to decreased SOD-1 activity.* Exp Neurol, 1997. **146**(1): p. 104-12.

43. Brown, D.R., R.S. Nicholas, and L. Canevari, *Lack of prion protein expression results in a neuronal phenotype sensitive to stress.* J Neurosci Res, 2002. **67**(2): p. 211-24.

44. Kim, B.H., et al., *The cellular prion protein (PrPC) prevents apoptotic neuronal cell death and mitochondrial dysfunction induced by serum deprivation.* Brain Res Mol Brain Res, 2004. **124**(1): p. 40-50.

45. Wong, B.S., et al., *Increased levels of oxidative stress markers detected in the brains of mice devoid of prion protein.* J Neurochem, 2001. **76**(2): p. 565-72.

46. Brown, D.R., et al., *The cellular prion protein binds copper in vivo.* Nature, 1997. **390**(6661): p. 684-7.

47. Jackson, G.S., et al., *Location and properties of metal-binding sites on the human prion protein.* Proc Natl Acad Sci U S A, 2001. **98**(15): p. 8531-5.

48. Kramer, M.L., et al., *Prion protein binds copper within the physiological concentration range.* J Biol Chem, 2001. **276**(20): p. 16711-9.

49. Pauly, P.C. and D.A. Harris, *Copper stimulates endocytosis of the prion protein.* J Biol Chem, 1998. **273**(50): p. 33107-10.

50. Stockel, J., et al., *Prion protein selectively binds copper(II) ions.* Biochemistry, 1998. **37**(20): p. 7185-93.

51. Walter, E.D., M. Chattopadhyay, and G.L. Millhauser, *The affinity of copper binding to the prion protein octarepeat domain: evidence for negative cooperativity.* Biochemistry, 2006. **45**(43): p. 13083-92.

52. Pan, K.M., et al., *Conversion of alpha-helices into beta-sheets features in the formation of the scrapie prion proteins.* Proc Natl Acad Sci U S A, 1993. **90**(23): p. 10962-6.

53. Prusiner, S.B., *Prions.* Proc Natl Acad Sci U S A, 1998. **95**(23): p. 13363-83.

54. Safar, J., et al., *Eight prion strains have PrP(Sc) molecules with different conformations.* Nat Med, 1998. **4**(10): p. 1157-65.

55. Raeber, A.J., et al., *Attempts to convert the cellular prion protein into the scrapie isoform in cell-free systems.* J Virol, 1992. **66**(10): p. 6155-63.

56. Jarrett, J.T. and P.T. Lansbury, Jr., *Seeding "one-dimensional crystallization" of amyloid: a pathogenic mechanism in Alzheimer's disease and scrapie?* Cell, 1993. **73**(6): p. 1055-8.

57. Saborio, G.P., et al., *Cell-lysate conversion of prion protein into its protease-resistant isoform suggests the participation of a cellular chaperone.* Biochem Biophys Res Commun, 1999. **258**(2): p. 470-5.

58. Abid, K. and C. Soto, *The intriguing prion disorders.* Cell Mol Life Sci, 2006. **63**(19-20): p. 2342-51.

59. Cordeiro, Y., et al., *DNA converts cellular prion protein into the beta-sheet conformation and inhibits prion peptide aggregation.* J Biol Chem, 2001. **276**(52): p. 49400-9.

60. Deleault, N.R., et al., *Protease-resistant prion protein amplification reconstituted with partially purified substrates and synthetic polyanions.* J Biol Chem, 2005. **280**(29): p. 26873-9.

61. Telling, G.C., et al., *Prion propagation in mice expressing human and chimeric PrP transgenes implicates the interaction of cellular PrP with another protein.* Cell, 1995. **83**(1): p. 79-90.

62. Kaneko, K., et al., *Evidence for protein X binding to a discontinuous epitope on the cellular prion protein during scrapie prion propagation.* Proc Natl Acad Sci U S A, 1997. **94**(19): p. 10069-74.

63. Simons, K. and E. Ikonen, *Functional rafts in cell membranes.* Nature, 1997. **387**(6633): p. 569-72.

64. Brown, D.A. and E. London, *Structure and function of sphingolipid- and cholesterol-rich membrane rafts.* J Biol Chem, 2000. **275**(23): p. 17221-4.

65. Hooper, N.M., *Detergent-insoluble glycosphingolipid/cholesterol-rich membrane domains, lipid rafts and caveolae (review).* Mol Membr Biol, 1999. **16**(2): p. 145-56.

66. van Keulen, L.J., M.E. Vromans, and F.G. van Zijderveld, *Early and late pathogenesis of natural scrapie infection in sheep.* Apmis, 2002. **110**(1): p. 23-32.

67. Heppner, F.L., et al., *Transepithelial prion transport by M cells.* Nat Med, 2001. **7**(9): p. 976-7.

68. Glaysher, B.R. and N.A. Mabbott, *Isolated lymphoid follicle maturation induces the development of follicular dendritic cells.* Immunology, 2007. **120**(3): p. 336-44.

69. Kitamoto, T., et al., *Abnormal isoform of prion protein accumulates in follicular dendritic cells in mice with Creutzfeldt-Jakob disease.* J Virol, 1991. **65**(11): p. 6292-5.

70. Blanquet-Grossard, F., et al., *Complement protein C1q recognizes a conformationally modified form of the prion protein.* Biochemistry, 2005. **44**(11): p. 4349-56.

71. Endres, R., et al., *Mature follicular dendritic cell networks depend on expression of lymphotoxin beta receptor by radioresistant stromal cells and of lymphotoxin beta and tumor necrosis factor by B cells.* J Exp Med, 1999. **189**(1): p. 159-68.

72. Mackay, F. and J.L. Browning, *Turning off follicular dendritic cells.* Nature, 1998. **395**(6697): p. 26-7.

73. Pasparakis, M., et al., *Immune and inflammatory responses in TNF alpha-deficient mice: a critical requirement for TNF alpha in the formation of primary B cell follicles, follicular dendritic cell networks and germinal centers, and in the maturation of the humoral immune response.* J Exp Med, 1996. **184**(4): p. 1397-411.

74. Glatzel, M., et al., *Sympathetic innervation of lymphoreticular organs is rate limiting for prion neuroinvasion.* Neuron, 2001. **31**(1): p. 25-34.

75. Chesebro, B., *Prion protein and the transmissible spongiform encephalopathy diseases.* Neuron, 1999. **24**(3): p. 503-6.

76. Rezaie, P. and P.L. Lantos, *Microglia and the pathogenesis of spongiform encephalopathies.* Brain Res Brain Res Rev, 2001. **35**(1): p. 55-72.

77. Wells, G.A., *Pathology of nonhuman spongiform encephalopathies: variations and their implications for pathogenesis.* Dev Biol Stand, 1993. **80**: p. 61-9.

78. Giese, A., et al., *Neuronal cell death in scrapie-infected mice is due to apoptosis.* Brain Pathol, 1995. **5**(3): p. 213-21.

79. Dron, M., et al., *Scrg1 is induced in TSE and brain injuries, and associated with autophagy.* Eur J Neurosci, 2005. **22**(1): p. 133-46.

80. Liberski, P.P. and M. Jaskolski, *Prion diseases: a dual view of the prion hypothesis as seen from a distance.* Acta Neurobiol Exp (Wars), 2002. **62**(3): p. 197-224; discussion 224-6.

81. Chiesa, R. and D.A. Harris, *Prion diseases: what is the neurotoxic molecule?* Neurobiol Dis, 2001. **8**(5): p. 743-63.

82. Della-Bianca, V., et al., *Neurotrophin p75 receptor is involved in neuronal damage by prion peptide-(106-126).* J Biol Chem, 2001. **276**(42): p. 38929-33.

83. Forloni, G., et al., *Neurotoxicity of a prion protein fragment.* Nature, 1993. **362**(6420): p. 543-6.

84. Hetz, C., et al., *Caspase-12 and endoplasmic reticulum stress mediate neurotoxicity of pathological prion protein.* Embo J, 2003. **22**(20): p. 5435-45.

85. Brown, D.R. and H.A. Kretzschmar, *Microglia and prion disease: a review.* Histol Histopathol, 1997. **12**(3): p. 883-92.

86. Giese, A., et al., *Role of microglia in neuronal cell death in prion disease.* Brain Pathol, 1998. **8**(3): p. 449-57.

87. Gonzalez-Scarano, F. and G. Baltuch, *Microglia as mediators of inflammatory and degenerative diseases.* Annu Rev Neurosci, 1999. **22**: p. 219-40.

88. Rogers, J., et al., *Microglia and inflammatory mechanisms in the clearance of amyloid beta peptide.* Glia, 2002. **40**(2): p. 260-9.

89. Streit, W.J., S.A. Walter, and N.A. Pennell, *Reactive microgliosis.* Prog Neurobiol, 1999. **57**(6): p. 563-81.

90. Gallo, V., et al., *Selective release of glutamate from cerebellar granule cells differentiating in culture.* Proc Natl Acad Sci U S A, 1982. **79**(24): p. 7919-23.

91. Choi, D.W., J.Y. Koh, and S. Peters, *Pharmacology of glutamate neurotoxicity in cortical cell culture: attenuation by NMDA antagonists.* J Neurosci, 1988. **8**(1): p. 185-96.

92. Brown, D.R. and C.M. Mohn, *Astrocytic glutamate uptake and prion protein expression.* Glia, 1999. **25**(3): p. 282-92.

93. Brown, D.R., B. Schmidt, and H.A. Kretzschmar, *A neurotoxic prion protein fragment enhances proliferation of microglia but not astrocytes in culture.* Glia, 1996. **18**(1): p. 59-67.

94. Forloni, G., et al., *A neurotoxic prion protein fragment induces rat astroglial proliferation and hypertrophy.* Eur J Neurosci, 1994. **6**(9): p. 1415-22.

95. Hafiz, F.B. and D.R. Brown, *A model for the mechanism of astrogliosis in prion disease.* Mol Cell Neurosci, 2000. **16**(3): p. 221-32.

96. Peyrin, J.M., et al., *Microglial cells respond to amyloidogenic PrP peptide by the production of inflammatory cytokines.* Neuroreport, 1999. **10**(4): p. 723-9.

97. Williams, A.E., et al., *Characterization of the microglial response in murine scrapie.* Neuropathol Appl Neurobiol, 1994. **20**(1): p. 47-55.

98. Betmouni, S., V.H. Perry, and J.L. Gordon, *Evidence for an early inflammatory response in the central nervous system of mice with scrapie.* Neuroscience, 1996. **74**(1): p. 1-5.

99. Fraser, H., et al., *Replication of scrapie in spleens of SCID mice follows reconstitution with wild-type mouse bone marrow.* J Gen Virol, 1996. **77 (Pt 8)**: p. 1935-40.

100. Lewicki, H., et al., *T cells infiltrate the brain in murine and human transmissible spongiform encephalopathies.* J Virol, 2003. **77**(6): p. 3799-808.

101. Brown, A.R., et al., *Inducible cytokine gene expression in the brain in the ME7/CV mouse model of scrapie is highly restricted, is at a strikingly low level relative to the degree of gliosis and occurs only late in disease.* J Gen Virol, 2003. **84**(Pt 9): p. 2605-11.

102. Burwinkel, M., et al., *Role of cytokines and chemokines in prion infections of the central nervous system.* Int J Dev Neurosci, 2004. **22**(7): p. 497-505.

103. Campbell, I.L., et al., *Activation of cerebral cytokine gene expression and its correlation with onset of reactive astrocyte and acute-phase response gene expression in scrapie.* J Virol, 1994. **68**(4): p. 2383-7.

104. Kim, J.I., et al., *Expression of cytokine genes and increased nuclear factor-kappa B activity in the brains of scrapie-infected mice.* Brain Res Mol Brain Res, 1999. **73**(1-2): p. 17-27.

105. Williams, A., et al., *Immunocytochemical appearance of cytokines, prostaglandin E2 and lipocortin-1 in the CNS during the incubation period of murine scrapie correlates with progressive PrP accumulations.* Brain Res, 1997. **754**(1-2): p. 171-80.

106. Schultz, J., et al., *Role of interleukin-1 in prion disease-associated astrocyte activation.* Am J Pathol, 2004. **165**(2): p. 671-8.

107. Sui, Y., et al., *Neuronal apoptosis is mediated by CXCL10 overexpression in simian human immunodeficiency virus encephalitis.* Am J Pathol, 2004. **164**(5): p. 1557-66.

108. Dheen, S.T., C. Kaur, and E.A. Ling, *Microglial activation and its implications in the brain diseases.* Curr Med Chem, 2007. **14**(11): p. 1189-97.

109. Beringue, V., P. Couvreur, and D. Dormont, *Involvement of macrophages in the pathogenesis of transmissible spongiform encephalopathies.* Dev Immunol, 2002. **9**(1): p. 19-27.

110. Perry, V.H., C. Cunningham, and D. Boche, *Atypical inflammation in the central nervous system in prion disease.* Curr Opin Neurol, 2002. **15**(3): p. 349-54.

111. Fadok, V.A., et al., *Regulation of macrophage cytokine production by phagocytosis of apoptotic and post-apoptotic cells.* Biochem Soc Trans, 1998. **26**(4): p. 653-6.

112. Gehrmann, J., et al., *Reactive microglia in cerebral ischaemia: an early mediator of tissue damage?* Neuropathol Appl Neurobiol, 1995. **21**(4): p. 277-89.

113. Rotshenker, S., *Microglia and macrophage activation and the regulation of complement-receptor-3 (CR3/MAC-1)-mediated myelin phagocytosis in injury and disease.* J Mol Neurosci, 2003. **21**(1): p. 65-72.

114. Barondes, S.H., et al., *Galectins: a family of animal beta-galactoside-binding lectins.* Cell, 1994. **76**(4): p. 597-8.

115. Kasai, K. and J. Hirabayashi, *Galectins: a family of animal lectins that decipher glycocodes.* J Biochem, 1996. **119**(1): p. 1-8.

116. Gabius, H.J., et al., *Association of galectin-1- but not galectin-3-dependent parameters with proliferation activity in human neuroblastomas and small cell lung carcinomas.* Anticancer Res, 2002. **22**(1A): p. 405-10.

117. Cooper, D.N. and S.H. Barondes, *Evidence for export of a muscle lectin from cytosol to extracellular matrix and for a novel secretory mechanism.* J Cell Biol, 1990. **110**(5): p. 1681-91.

118. Hughes, R.C., *Secretion of the galectin family of mammalian carbohydrate-binding proteins.* Biochim Biophys Acta, 1999. **1473**(1): p. 172-85.

119. Sato, S., I. Burdett, and R.C. Hughes, *Secretion of the baby hamster kidney 30-kDa galactose-binding lectin from polarized and nonpolarized cells: a pathway independent of the endoplasmic reticulum-Golgi complex.* Exp Cell Res, 1993. **207**(1): p. 8-18.

120. Hirabayashi, J. and K. Kasai, *The family of metazoan metal-independent beta-galactoside-binding lectins: structure, function and molecular evolution.* Glycobiology, 1993. **3**(4): p. 297-304.

121. Ho, M.K. and T.A. Springer, *Mac-2, a novel 32,000 Mr mouse macrophage subpopulation-specific antigen defined by monoclonal antibodies.* J Immunol, 1982. **128**(3): p. 1221-8.

122. Houzelstein, D., et al., *Phylogenetic analysis of the vertebrate galectin family.* Mol Biol Evol, 2004. **21**(7): p. 1177-87.

123. Lindstedt, R., et al., *Apical secretion of a cytosolic protein by Madin-Darby canine kidney cells. Evidence for polarized release of an endogenous lectin by a nonclassical secretory pathway.* J Biol Chem, 1993. **268**(16): p. 11750-7.

124. Nickel, W., *The mystery of nonclassical protein secretion. A current view on cargo proteins and potential export routes.* Eur J Biochem, 2003. **270**(10): p. 2109-19.

125. Rabinovich, G.A., et al., *Galectins and their ligands: amplifiers, silencers or tuners of the inflammatory response?* Trends Immunol, 2002. **23**(6): p. 313-20.

126. Birdsall, B., et al., *NMR solution studies of hamster galectin-3 and electron microscopic visualization of surface-adsorbed complexes: evidence for interactions between the N- and C-terminal domains.* Biochemistry, 2001. **40**(15): p. 4859-66.

127. Hsu, D.K., R.I. Zuberi, and F.T. Liu, *Biochemical and biophysical characterization of human recombinant IgE-binding protein, an S-type animal lectin.* J Biol Chem, 1992. **267**(20): p. 14167-74.

128. Ochieng, J., et al., *Structure-function relationship of a recombinant human galactoside-binding protein.* Biochemistry, 1993. **32**(16): p. 4455-60.

129. Sato, S. and R.C. Hughes, *Binding specificity of a baby hamster kidney lectin for H type I and II chains, polylactosamine glycans, and appropriately glycosylated forms of laminin and fibronectin.* J Biol Chem, 1992. **267**(10): p. 6983-90.

130. Seetharaman, J., et al., *X-ray crystal structure of the human galectin-3 carbohydrate recognition domain at 2.1-A resolution.* J Biol Chem, 1998. **273**(21): p. 13047-52.

131. Yang, R.Y., D.K. Hsu, and F.T. Liu, *Expression of galectin-3 modulates T-cell growth and apoptosis.* Proc Natl Acad Sci U S A, 1996. **93**(13): p. 6737-42.

132. Barboni, E.A., et al., *Molecular modeling and mutagenesis studies of the N-terminal domains of galectin-3: evidence for participation with the C-terminal carbohydrate recognition domain in oligosaccharide binding.* Glycobiology, 2000. **10**(11): p. 1201-8.

133. Mehul, B. and R.C. Hughes, *Plasma membrane targetting, vesicular budding and release of galectin 3 from the cytoplasm of mammalian cells during secretion.* J Cell Sci, 1997. **110 (Pt 10)**: p. 1169-78.

134. Bao, Q. and R.C. Hughes, *Galectin-3 expression and effects on cyst enlargement and tubulogenesis in kidney epithelial MDCK cells cultured in three-dimensional matrices in vitro.* J Cell Sci, 1995. **108 (Pt 8)**: p. 2791-800.

135. Flotte, T.J., T.A. Springer, and G.J. Thorbecke, *Dendritic cell and macrophage staining by monoclonal antibodies in tissue sections and epidermal sheets.* Am J Pathol, 1983. **111**(1): p. 112-24.

136. Kasper, M. and R.C. Hughes, *Immunocytochemical evidence for a modulation of galectin 3 (Mac-2), a carbohydrate binding protein, in pulmonary fibrosis.* J Pathol, 1996. **179**(3): p. 309-16.

137. Craig, S.S., et al., *Immunoelectron microscopic localization of galectin-3, an IgE binding protein, in human mast cells and basophils.* Anat Rec, 1995. **242**(2): p. 211-9.

138. Frigeri, L.G., R.I. Zuberi, and F.T. Liu, *Epsilon BP, a beta-galactoside-binding animal lectin, recognizes IgE receptor (Fc epsilon RI) and activates mast cells.* Biochemistry, 1993. **32**(30): p. 7644-9.

139. Liu, F.T., et al., *Expression and function of galectin-3, a beta-galactoside-binding lectin, in human monocytes and macrophages.* Am J Pathol, 1995. **147**(4): p. 1016-28.

140. Saada, A., F. Reichert, and S. Rotshenker, *Granulocyte macrophage colony stimulating factor produced in lesioned peripheral nerves induces the up-regulation of cell surface expression of MAC-2 by macrophages and Schwann cells.* J Cell Biol, 1996. **133**(1): p. 159-67.

141. Truong, M.J., et al., *Human neutrophils express immunoglobulin E (IgE)-binding proteins (Mac-2/epsilon BP) of the S-type lectin family: role in IgE-dependent activation.* J Exp Med, 1993. **177**(1): p. 243-8.

142. Truong, M.J., et al., *IgE-binding molecules (Mac-2/epsilon BP) expressed by human eosinophils. Implication in IgE-dependent eosinophil cytotoxicity.* Eur J Immunol, 1993. **23**(12): p. 3230-5.

143. Dumic, J., S. Dabelic, and M. Flogel, *Galectin-3: an open-ended story.* Biochim Biophys Acta, 2006. **1760**(4): p. 616-35.

144. Hamann, K.K., et al., *Expression of carbohydrate binding protein 35 in human fibroblasts: variations in the levels of mRNA, protein, and isoelectric species as a function of replicative competence.* Exp Cell Res, 1991. **196**(1): p. 82-91.

145. Hubert, M., et al., *Intranuclear distribution of galectin-3 in mouse 3T3 fibroblasts: comparative analyses by immunofluorescence and immunoelectron microscopy.* Exp Cell Res, 1995. **220**(2): p. 397-406.

146. Moutsatsos, I.K., J.M. Davis, and J.L. Wang, *Endogenous lectins from cultured cells: subcellular localization of carbohydrate-binding protein 35 in 3T3 fibroblasts.* J Cell Biol, 1986. **102**(2): p. 477-83.

147. Moutsatsos, I.K., et al., *Endogenous lectins from cultured cells: nuclear localization of carbohydrate-binding protein 35 in proliferating 3T3 fibroblasts.* Proc Natl Acad Sci U S A, 1987. **84**(18): p. 6452-6.

148. Openo, K.P., et al., *Galectin-3 expression and subcellular localization in senescent human fibroblasts.* Exp Cell Res, 2000. **255**(2): p. 278-90.

149. Elad-Sfadia, G., et al., *Galectin-3 augments K-Ras activation and triggers a Ras signal that attenuates ERK but not phosphoinositide 3-kinase activity.* J Biol Chem, 2004. **279**(33): p. 34922-30.

150. Lee, Y.J., et al., *Reconstitution of galectin-3 alters glutathione content and potentiates TRAIL-induced cytotoxicity by dephosphorylation of Akt.* Exp Cell Res, 2003. **288**(1): p. 21-34.

151. Liu, F.T., *Galectins: novel anti-inflammatory drug targets.* Expert Opin Ther Targets, 2002. **6**(4): p. 461-8.

152. Liu, L., et al., *Nucling mediates apoptosis by inhibiting expression of galectin-3 through interference with nuclear factor kappaB signalling.* Biochem J, 2004. **380**(Pt 1): p. 31-41.

153. Oka, N., et al., *Galectin-3 inhibits tumor necrosis factor-related apoptosis-inducing ligand-induced apoptosis by activating Akt in human bladder carcinoma cells.* Cancer Res, 2005. **65**(17): p. 7546-53.

154. Shalom-Feuerstein, R., et al., *Galectin-3 regulates a molecular switch from N-Ras to K-Ras usage in human breast carcinoma cells.* Cancer Res, 2005. **65**(16): p. 7292-300.

155. Lin, H.M., et al., *Galectin-3 enhances cyclin D(1) promoter activity through SP1 and a cAMP-responsive element in human breast epithelial cells.* Oncogene, 2002. **21**(52): p. 8001-10.

156. Park, J.W., et al., *Association of galectin-1 and galectin-3 with Gemin4 in complexes containing the SMN protein.* Nucleic Acids Res, 2001. **29**(17): p. 3595-602.

157. Pellizzoni, L., et al., *A novel function for SMN, the spinal muscular atrophy disease gene product, in pre-mRNA splicing.* Cell, 1998. **95**(5): p. 615-24.

158. Ochieng, J., V. Furtak, and P. Lukyanov, *Extracellular functions of galectin-3.* Glycoconj J, 2004. **19**(7-9): p. 527-35.

159. Dong, S. and R.C. Hughes, *Macrophage surface glycoproteins binding to galectin-3 (Mac-2-antigen).* Glycoconj J, 1997. **14**(2): p. 267-74.

160. Sano, H., et al., *Human galectin-3 is a novel chemoattractant for monocytes and macrophages.* J Immunol, 2000. **165**(4): p. 2156-64.

161. Fukumori, T., et al., *Endogenous galectin-3 determines the routing of CD95 apoptotic signaling pathways.* Cancer Res, 2004. **64**(10): p. 3376-9.

162. Nakahara, S., N. Oka, and A. Raz, *On the role of galectin-3 in cancer apoptosis.* Apoptosis, 2005. **10**(2): p. 267-75.

163. Feuk-Lagerstedt, E., et al., *Identification of CD66a and CD66b as the major galectin-3 receptor candidates in human neutrophils.* J Immunol, 1999. **163**(10): p. 5592-8.

164. Demetriou, M., et al., *Negative regulation of T-cell activation and autoimmunity by Mgat5 N-glycosylation.* Nature, 2001. **409**(6821): p. 733-9.

165. Sacchettini, J.C., L.G. Baum, and C.F. Brewer, *Multivalent protein-carbohydrate interactions. A new paradigm for supermolecular assembly and signal transduction.* Biochemistry, 2001. **40**(10): p. 3009-15.

166. Mandrell, R.E., et al., *Possible interaction between animal lectins and bacterial carbohydrates.* Methods Enzymol, 1994. **236**: p. 231-54.

167. Mey, A., et al., *The animal lectin galectin-3 interacts with bacterial lipopolysaccharides via two independent sites.* J Immunol, 1996. **156**(4): p. 1572-7.

168. Gupta, S.K., et al., *Pseudomonas aeruginosa lipopolysaccharide binds galectin-3 and other human corneal epithelial proteins.* Infect Immun, 1997. **65**(7): p. 2747-53.

169. Beatty, W.L., et al., *Association of a macrophage galactoside-binding protein with Mycobacterium-containing phagosomes.* Cell Microbiol, 2002. **4**(3): p. 167-76.

170. Sano, H., et al., *Critical role of galectin-3 in phagocytosis by macrophages.* J Clin Invest, 2003. **112**(3): p. 389-97.

171. Reichert, F. and S. Rotshenker, *Galectin-3/MAC-2 in experimental allergic encephalomyelitis.* Exp Neurol, 1999. **160**(2): p. 508-14.

172. Hsu, D.K., et al., *Targeted disruption of the galectin-3 gene results in attenuated peritoneal inflammatory responses.* Am J Pathol, 2000. **156**(3): p. 1073-83.

173. Zuberi, R.I., et al., *Critical role for galectin-3 in airway inflammation and bronchial hyperresponsiveness in a murine model of asthma.* Am J Pathol, 2004. **165**(6): p. 2045-53.

174. Pesheva, P., et al., *Murine microglial cells express functionally active galectin-3 in vitro.* J Neurosci Res, 1998. **51**(1): p. 49-57.

175. Reichert, F., A. Saada, and S. Rotshenker, *Peripheral nerve injury induces Schwann cells to express two macrophage phenotypes: phagocytosis and the galactose-specific lectin MAC-2.* J Neurosci, 1994. **14**(5 Pt 2): p. 3231-45.

176. Yang, J.W., et al., *Mass spectrometrical analysis of galectin proteins in primary rat cerebellar astrocytes.* Neurochem Res, 2006. **31**(7): p. 945-55.

177. Daude, N., M. Marella, and J. Chabry, *Specific inhibition of pathological prion protein accumulation by small interfering RNAs.* J Cell Sci, 2003. **116**(Pt 13): p. 2775-9.

178. Mallucci, G., et al., *Depleting neuronal PrP in prion infection prevents disease and reverses spongiosis.* Science, 2003. **302**(5646): p. 871-4.

179. Enari, M., E. Flechsig, and C. Weissmann, *Scrapie prion protein accumulation by scrapie-infected neuroblastoma cells abrogated by exposure to a prion protein antibody.* Proc Natl Acad Sci U S A, 2001. **98**(16): p. 9295-9.

180. Heppner, F.L., et al., *Prevention of scrapie pathogenesis by transgenic expression of anti-prion protein antibodies.* Science, 2001. **294**(5540): p. 178-82.

181. Barret, A., et al., *Evaluation of quinacrine treatment for prion diseases.* J Virol, 2003. **77**(15): p. 8462-9.

182. Benito-Leon, J., *Combined quinacrine and chlorpromazine therapy in fatal familial insomnia.* Clin Neuropharmacol, 2004. **27**(4): p. 201-3.

183. Collins, S.J., et al., *Quinacrine does not prolong survival in a murine Creutzfeldt-Jakob disease model.* Ann Neurol, 2002. **52**(4): p. 503-6.

184. Doh-ura, K., et al., *Treatment of transmissible spongiform encephalopathy by intraventricular drug infusion in animal models.* J Virol, 2004. **78**(10): p. 4999-5006.

185. Kocisko, D.A., et al., *Evaluation of new cell culture inhibitors of protease-resistant prion protein against scrapie infection in mice.* J Gen Virol, 2004. **85**(Pt 8): p. 2479-83.

186. Taraboulos, A., et al., *Cholesterol depletion and modification of COOH-terminal targeting sequence of the prion protein inhibit formation of the scrapie isoform.* J Cell Biol, 1995. **129**(1): p. 121-32.

187. Brown, M.S. and J.L. Goldstein, *Lowering plasma cholesterol by raising LDL receptors.* N Engl J Med, 1981. **305**(9): p. 515-7.

188. Weitz-Schmidt, G., *Statins as anti-inflammatory agents.* Trends Pharmacol Sci, 2002. **23**(10): p. 482-6.

189. Weitz-Schmidt, G., et al., *Statins selectively inhibit leukocyte function antigen-1 by binding to a novel regulatory integrin site.* Nat Med, 2001. **7**(6): p. 687-92.

190. Youssef, S., et al., *The HMG-CoA reductase inhibitor, atorvastatin, promotes a Th2 bias and reverses paralysis in central nervous system autoimmune disease.* Nature, 2002. **420**(6911): p. 78-84.

191. Amarenco, P., et al., *Design and baseline characteristics of the stroke prevention by aggressive reduction in cholesterol levels (SPARCL) study.* Cerebrovasc Dis, 2003. **16**(4): p. 389-95.

192. Thelen, K.M., et al., *Brain cholesterol synthesis in mice is affected by high dose of simvastatin but not of pravastatin.* J Pharmacol Exp Ther, 2006. **316**(3): p. 1146-52.

193. Riemer, C., et al., *Gene expression profiling of scrapie-infected brain tissue.* Biochem Biophys Res Commun, 2004. **323**(2): p. 556-64.

194. Marella, M. and J. Chabry, *Neurons and astrocytes respond to prion infection by inducing microglia recruitment.* J Neurosci, 2004. **24**(3): p. 620-7.

195. Chen, J.W., et al., *Identification of two lysosomal membrane glycoproteins.* J Cell Biol, 1985. **101**(1): p. 85-95.

196. Eskelinen, E.L., *Roles of LAMP-1 and LAMP-2 in lysosome biogenesis and autophagy.* Mol Aspects Med, 2006. **27**(5-6): p. 495-502.

197. Tanaka, Y., et al., *Accumulation of autophagic vacuoles and cardiomyopathy in LAMP-2-deficient mice.* Nature, 2000. **406**(6798): p. 902-6.

198. Asanuma, K., et al., *MAP-LC3, a promising autophagosomal marker, is processed during the differentiation and recovery of podocytes from PAN nephrosis.* Faseb J, 2003. **17**(9): p. 1165-7.

199. Kabeya, Y., et al., *LC3, a mammalian homologue of yeast Apg8p, is localized in autophagosome membranes after processing.* Embo J, 2000. **19**(21): p. 5720-8.

200. Zhu, J.H., et al., *Regulation of autophagy by extracellular signal-regulated protein kinases during 1-methyl-4-phenylpyridinium-induced cell death.* Am J Pathol, 2007. **170**(1): p. 75-86.

201. Mizushima, N., Y. Ohsumi, and T. Yoshimori, *Autophagosome formation in mammalian cells.* Cell Struct Funct, 2002. **27**(6): p. 421-9.

202. Pricci, F., et al., *Role of galectin-3 as a receptor for advanced glycosylation end products.* Kidney Int Suppl, 2000. **77**: p. S31-9.

203. Vlassara, H., et al., *Identification of galectin-3 as a high-affinity binding protein for advanced glycation end products (AGE): a new member of the AGE-receptor complex.* Mol Med, 1995. **1**(6): p. 634-46.

204. Choi, Y.G., et al., *Nonenzymatic glycation at the N terminus of pathogenic prion protein in transmissible spongiform encephalopathies.* J Biol Chem, 2004. **279**(29): p. 30402-9.

205. Riemer, C., et al., *Identification of upregulated genes in scrapie-infected brain tissue.* J Virol, 2000. **74**(21): p. 10245-8.

206. Xiang, W., et al., *Cerebral gene expression profiles in sporadic Creutzfeldt-Jakob disease.* Ann Neurol, 2005. **58**(2): p. 242-57.

207. Bate, C., et al., *Squalestatin cures prion-infected neurons and protects against prion neurotoxicity.* J Biol Chem, 2004. **279**(15): p. 14983-90.

208. Aucouturier, P., et al., *Infected splenic dendritic cells are sufficient for prion transmission to the CNS in mouse scrapie.* J Clin Invest, 2001. **108**(5): p. 703-8.

209. Kimberlin, R.H. and C.A. Walker, *Intraperitoneal infection with scrapie is established within minutes of injection and is non-specifically enhanced by a variety of different drugs.* Arch Virol, 1990. **112**(1-2): p. 103-14.

210. Manuelidis, L., et al., *Follicular dendritic cells and dissemination of Creutzfeldt-Jakob disease.* J Virol, 2000. **74**(18): p. 8614-22.

211. Sethi, S., et al., *Role of the CD8+ dendritic cell subset in transmission of prions.* J Virol, 2007. **81**(9): p. 4877-80.

212. Laszlo, L., et al., *Lysosomes as key organelles in the pathogenesis of prion encephalopathies.* J Pathol, 1992. **166**(4): p. 333-41.

213. Kopacek, J., et al., *Upregulation of the genes encoding lysosomal hydrolases, a perforin-like protein, and peroxidases in the brains of mice affected with an experimental prion disease.* J Virol, 2000. **74**(1): p. 411-7.

214. Nixon, R.A., A.M. Cataldo, and P.M. Mathews, *The endosomal-lysosomal system of neurons in Alzheimer's disease pathogenesis: a review.* Neurochem Res, 2000. **25**(9-10): p. 1161-72.

215. Klionsky, D.J., *The molecular machinery of autophagy: unanswered questions.* J Cell Sci, 2005. **118**(Pt 1): p. 7-18.

216. Sikorska, B., et al., *Autophagy is a part of ultrastructural synaptic pathology in Creutzfeldt-Jakob disease: a brain biopsy study.* Int J Biochem Cell Biol, 2004. **36**(12): p. 2563-73.

217. Hara, T., et al., *Suppression of basal autophagy in neural cells causes neurodegenerative disease in mice.* Nature, 2006. **441**(7095): p. 885-9.

218. Komatsu, M., et al., *Loss of autophagy in the central nervous system causes neurodegeneration in mice.* Nature, 2006. **441**(7095): p. 880-4.

219. Stern, D.M., et al., *Receptor for advanced glycation endproducts (RAGE) and the complications of diabetes.* Ageing Res Rev, 2002. **1**(1): p. 1-15.

220. Horiuchi, S., Y. Sakamoto, and M. Sakai, *Scavenger receptors for oxidized and glycated proteins.* Amino Acids, 2003. **25**(3-4): p. 283-92.

221. Ohgami, N., et al., *CD36, serves as a receptor for advanced glycation endproducts (AGE).* J Diabetes Complications, 2002. **16**(1): p. 56-9.

222. Horiuchi, S., et al., *Advanced glycation end products and their recognition by macrophage and macrophage-derived cells.* Diabetes, 1996. **45 Suppl 3**: p. S73-6.

223. Ohgami, N., et al., *Cd36, a member of the class b scavenger receptor family, as a receptor for advanced glycation end products.* J Biol Chem, 2001. **276**(5): p. 3195-202.

224. Stitt, A.W., et al., *Advanced glycation end products (AGEs) co-localize with AGE receptors in the retinal vasculature of diabetic and of AGE-infused rats.* Am J Pathol, 1997. **150**(2): p. 523-31.

225. Brownlee, M., *Advanced protein glycosylation in diabetes and aging.* Annu Rev Med, 1995. **46**: p. 223-34.

226. Gomes, R., et al., *Argpyrimidine, a methylglyoxal-derived advanced glycation end-product in familial amyloidotic polyneuropathy.* Biochem J, 2005. **385**(Pt 2): p. 339-45.

227. Ulrich, P. and A. Cerami, *Protein glycation, diabetes, and aging.* Recent Prog Horm Res, 2001. **56**: p. 1-21.

228. Bank, R.A., et al., *Ageing and zonal variation in post-translational modification of collagen in normal human articular cartilage. The age-related increase in non-enzymatic glycation affects biomechanical properties of cartilage.* Biochem J, 1998. **330 (Pt 1)**: p. 345-51.

229. DeGroot, J., et al., *Age-related decrease in proteoglycan synthesis of human articular chondrocytes: the role of nonenzymatic glycation.* Arthritis Rheum, 1999. **42**(5): p. 1003-9.

230. Dunn, J.A., et al., *Age-dependent accumulation of N epsilon-(carboxymethyl)lysine and N epsilon-(carboxymethyl)hydroxylysine in human skin collagen.* Biochemistry, 1991. **30**(5): p. 1205-10.

231. Di Mario, U. and G. Pugliese, *15th Golgi lecture: from hyperglycaemia to the dysregulation of vascular remodelling in diabetes.* Diabetologia, 2001. **44**(6): p. 674-92.

232. Iacobini, C., et al., *Role of galectin-3 in diabetic nephropathy.* J Am Soc Nephrol, 2003. **14**(8 Suppl 3): p. S264-70.

233. Drinda, S., et al., *Identification of the advanced glycation end products N(epsilon)-carboxymethyllysine in the synovial tissue of patients with rheumatoid arthritis.* Ann Rheum Dis, 2002. **61**(6): p. 488-92.

234. Iacobini, C., et al., *Galectin-3/AGE-receptor 3 knockout mice show accelerated AGE-induced glomerular injury: evidence for a protective role of galectin-3 as an AGE receptor.* Faseb J, 2004. **18**(14): p. 1773-5.

235. Safar, J.G., et al., *Human prions and plasma lipoproteins.* Proc Natl Acad Sci U S A, 2006. **103**(30): p. 11312-7.

236. Zhu, W., et al., *The role of galectin-3 in endocytosis of advanced glycation end products and modified low density lipoproteins.* Biochem Biophys Res Commun, 2001. **280**(4): p. 1183-8.

237. Vitek, M.P., et al., *Advanced glycation end products contribute to amyloidosis in Alzheimer disease.* Proc Natl Acad Sci U S A, 1994. **91**(11): p. 4766-70.

238. Yan, S.D., et al., *Glycated tau protein in Alzheimer disease: a mechanism for induction of oxidant stress.* Proc Natl Acad Sci U S A, 1994. **91**(16): p. 7787-91.

239. Yan, S.D., et al., *An intracellular protein that binds amyloid-beta peptide and mediates neurotoxicity in Alzheimer's disease.* Nature, 1997. **389**(6652): p. 689-95.

240. Brown, D., et al., *Early loss of dendritic spines in murine scrapie revealed by confocal analysis.* Neuroreport, 2001. **12**(1): p. 179-83.

241. Cunningham, C., et al., *Neuropathologically distinct prion strains give rise to similar temporal profiles of behavioral deficits.* Neurobiol Dis, 2005. **18**(2): p. 258-69.

242. McFarland, D. and J. Hotchin, *Early behavioral abnormalities in mice due to scrapie virus encephalopathy.* Biol Psychiatry, 1980. **15**(1): p. 37-44.

243. Suckling, A.J., et al., *Motor activity changes in scrapie-affected mice.* Br J Exp Pathol, 1976. **57**(6): p. 742-6.

244. Steimle, V., et al., *Complementation cloning of an MHC class II transactivator mutated in hereditary MHC class II deficiency (or bare lymphocyte syndrome).* Cell, 1993. **75**(1): p. 135-46.

245. Steimle, V., et al., *Regulation of MHC class II expression by interferon-gamma mediated by the transactivator gene CIITA.* Science, 1994. **265**(5168): p. 106-9.

246. Bjorkhem, I. and S. Meaney, *Brain cholesterol: long secret life behind a barrier.* Arterioscler Thromb Vasc Biol, 2004. **24**(5): p. 806-15.

247. Brown, M.S. and J.L. Goldstein, *Multivalent feedback regulation of HMG CoA reductase, a control mechanism coordinating isoprenoid synthesis and cell growth.* J Lipid Res, 1980. **21**(5): p. 505-17.

248. Cole, S.L. and R. Vassar, *Isoprenoids and Alzheimer's disease: a complex relationship.* Neurobiol Dis, 2006. **22**(2): p. 209-22.

249. Cox, A.D. and C.J. Der, *Farnesyltransferase inhibitors and cancer treatment: targeting simply Ras?* Biochim Biophys Acta, 1997. **1333**(1): p. F51-71.

250. Zhang, F.L. and P.J. Casey, *Protein prenylation: molecular mechanisms and functional consequences.* Annu Rev Biochem, 1996. **65**: p. 241-69.

251. Neuhaus, O., et al., *Are statins a treatment option for multiple sclerosis?* Lancet Neurol, 2004. **3**(6): p. 369-71.

252. Todd, N.V., et al., *Cerebroventricular infusion of pentosan polysulphate in human variant Creutzfeldt-Jakob disease.* J Infect, 2005. **50**(5): p. 394-6.

253. Demaimay, R., et al., *Late treatment with polyene antibiotics can prolong the survival time of scrapie-infected animals.* J Virol, 1997. **71**(12): p. 9685-9.

254. Manuelidis, L., W. Fritch, and I. Zaitsev, *Dapsone to delay symptoms in Creutzfeldt-Jakob disease.* Lancet, 1998. **352**(9126): p. 456.

255. Guenther, K., et al., *Early behavioural changes in scrapie-affected mice and the influence of dapsone.* Eur J Neurosci, 2001. **14**(2): p. 401-9.

256. Masullo, C., et al., *Failure to ameliorate Creutzfeldt-Jakob disease with amphotericin B therapy.* J Infect Dis, 1992. **165**(4): p. 784-5.

257. Sabra, R. and R.A. Branch, *Amphotericin B nephrotoxicity.* Drug Saf, 1990. **5**(2): p. 94-108.

258. Klotz, U., *Pharmacological comparison of the statins.* Arzneimittelforschung, 2003. **53**(9): p. 605-11.

259. Forloni, G., et al., *Tetracyclines affect prion infectivity.* Proc Natl Acad Sci U S A, 2002. **99**(16): p. 10849-54.

260. Herkenham, M., et al., *Cannabinoid receptor localization in brain.* Proc Natl Acad Sci U S A, 1990. **87**(5): p. 1932-6.

261. Westlake, T.M., et al., *Cannabinoid receptor binding and messenger RNA expression in human brain: an in vitro receptor autoradiography and in situ hybridization histochemistry study of normal aged and Alzheimer's brains.* Neuroscience, 1994. **63**(3): p. 637-52.

262. Howlett, A.C., *The cannabinoid receptors.* Prostaglandins Other Lipid Mediat, 2002. **68-69**: p. 619-31.

263. Nunez, E., et al., *Cannabinoid CB2 receptors are expressed by perivascular microglial cells in the human brain: an immunohistochemical study.* Synapse, 2004. **53**(4): p. 208-13.

264. Franklin, A. and N. Stella, *Arachidonylcyclopropylamide increases microglial cell migration through cannabinoid CB2 and abnormal-cannabidiol-sensitive receptors.* Eur J Pharmacol, 2003. **474**(2-3): p. 195-8.

265. Maresz, K., et al., *Modulation of the cannabinoid CB2 receptor in microglial cells in response to inflammatory stimuli.* J Neurochem, 2005. **95**(2): p. 437-45.

266. Jackson, S.J., et al., *Cannabinoids and neuroprotection in CNS inflammatory disease.* J Neurol Sci, 2005. **233**(1-2): p. 21-5.

267. Pryce, G., et al., *Cannabinoids inhibit neurodegeneration in models of multiple sclerosis.* Brain, 2003. **126**(Pt 10): p. 2191-202.

268. Luhr, K.M., et al., *Cathepsin B and L are involved in degradation of prions in GT1-1 neuronal cells.* Neuroreport, 2004. **15**(10): p. 1663-7.

269. Zhang, Y., et al., *Up-regulation of cathepsin B and cathepsin L activities in scrapie-infected mouse Neuro2a cells.* J Gen Virol, 2003. **84**(Pt 8): p. 2279-83.

270. Sarkar, S., et al., *Lithium induces autophagy by inhibiting inositol monophosphatase.* J Cell Biol, 2005. **170**(7): p. 1101-11.

7 Appendix

7.1 Abbreviation

24S-OH-chol	24S-hydroxycholesterol
˚C	Degree Celsius
µl	Microliter
µm	Micrometer
Aβ	beta-Amyloid
AGEs	Advanced glycation endproducts
AGE-R1	Advanced glycation endproducts receptor 1
AGE-R2	Advanced glycation endproducts receptor 2
Atg5	Autophagy gene 5
BBB	Blood Brain Barrier
BSE	Bovine Spongiform Encephalopathy
CEL	Carboxyethyllysine
CHO	Glycosylation
CJD	Creutzfeldt-Jacob Disease
CML	Carboxymethyllysine
CNS	Central Nervous System
CR3	Complement receptor-3
CRD	Carbohydrate-Recognition Domain
CWD	Chronic Wasting Disease
dpi	Days Postinfection
EAE	Experimental allergic encephalomyelitis
ELS	Endosomal/lysosomal system
ER	Endoplasmic Reticulum
FDCs	Follicular Dendritic Cells
FFI	Fatal Familial Insomnia
FPP	Farnesyl pyrophosphate
FSE	Feline Spongiform Encephalopathy
Galectin-3$^{-/-}$	Galectin-3 Deficiency
GALT	Gut-Associated Lymphoid Tissue

GB	Golgi Body
GCs	Germinal Centers
GFAP	Glial Fibrillary Acidic Protein
GGPP	Geranylgeranyl pyrophosphate
GPI	Glycosylphosphatidylinositol
GSS	Gerstmann-Sträussler-Scheinker-Syndrome
HMG-CoA	3-hydroxymethyl-3-glutaryl coenzyme A
HMG-CoAR	3-hydroxymethyl-3-glutaryl coenzyme A reductase
i.c.	Intracerebral
ILF	Isolated Lymphoid Follicle
i.p.	Intraperitoneal
kDa	Kilodalton
kg	Kilogram
LAPTm5	Lysosome-associated multitransmembrane protein
LC3-I	Microtubule-Associated Protein 1 Light Chain 3 (precursor)
LC3-II	Microtubule-Associated Protein 1 Light Chain 3 (active form)
LDL	Low-density lipoprotein
LFA-1	Leukocyte function antigen-1
LPS	Lippopolysaccharides
LT- β	Lymphotoxin-β
Min	Minute
MHC-II	Major Histocompatibilty Complex Class II
PAMPs	Pathogen Associated Molecular Patterns
PNS	Peripheral Nervous System
PPS	Pentosan Polysulfate
PRR	Pattern Recognitions Receptor
PrP^{c}	Cellular form of Prion Protein
PrP^{Sc}	Scrapie form of Prion Protein
PRNP	Prion Protein Gene
PTA	Phosphohtug acid
RAGE	Receptor of Advanced Glycation Endproducts

Sec	Second
SMN	Survival of Motor Neuron Protein
TIA	Transient Ischemic Attack
TCR	T-Cell Receptor
TGFβ1	Transforming Growth Factor-β
TME	Transmissible Mink Encephalopathy
TNF-α	Tumor Necrosis Factor-α
TSE	Transmissible Spongiform Encephalopathy
UV	Ultra-Violet
vCJD	variant Creutzfeldt-Jacob Disease
WT	Wildtype

7.2 List of Diagrams

7.3 List of Figures

7.4 List of Tables

8 List of Publications

1. Riemer, C., et al., *Accelerated prion replication in, but prolonged survival times of, prion-infected CXCR3-/- mice.* J Virol, 2008. **82**(24): p. 12464-71.

2. Riemer, C., et al., *Evaluation of drugs for treatment of prion infections of the central nervous system.* J Gen Virol, 2008. **89**(Pt 2): p. 594-7.

3. Mok, S.W., et al., *Role of galectin-3 in prion infections of the CNS.* Biochem Biophys Res Commun, 2007. **359**(3): p. 672-8.

4. Mok, S.W., et al., *Simvastatin prolongs survival times in prion infections of the central nervous system.* Biochem Biophys Res Commun, 2006. **348**(2): p. 697-702.

5. Riemer, C., et al., *3-Methyl-4-chlorophenol for prion decontamination of medical devices.* Infect Control Hosp Epidemiol, 2006. **27**(7): p. 778-80.